SUPPORTING INFORMATION

Different Roles of Myocardial ROCK1 and ROCK2 in Cardiac Dysfunction and Post-Capillary Pulmonary Hypertension in Mice

Shinichiro Sunamura MD[1]; Kimio Satoh, MD, PhD[1]; Ryo Kurosawa, MD[1]; Tomohiro Ohtsuki MD[1]; Nobuhiro Kikuchi, MD, PhD[1]; Md. Elias-Al-Mamun, PhD[1]; Toru Shimizu, MD, PhD[1]; Shohei Ikeda, MD, PhD[1]; Kota Suzuki, MD[1]; Taijyu Satoh, MD[1]; Junichi Omura, MD, PhD[1]; Masamichi Nogi, MD[1]; Kazuhiko Numano MD[1]; Mohammad Abdul Hai Siddique, PhD[1]; Satoshi Miyata, PhD[1]; Masahito Miura, MD, PhD[2]; Hiroaki Shimokawa, MD, PhD[1]

[1]Department of Cardiovascular Medicine, Tohoku University Graduate School of Medicine, Sendai, Japan; [2]Department of Clinical Physiology, Health Science, Tohoku University Graduate School of Medicine, Sendai, Japan

Supplementary Methods

Generation and Genotyping of Cardiac-specific ROCK1-deficient Mice and Cardiac-specific ROCK2-deficient Mice

For generation of *Rock1*-floxed mice, the targeting vector was generated by flanking exon 5 of the mouse *Rock1* gene with 2 loxP sites to induce Cre-mediated deletion of exon 5. The single loxP site is inserted 5' to exon 5 and loxP/FRT-flanked neomycin (Neo) resistance cassette was inserted 3' to exon 5. The targeting vector was electroporated into RENKA embryonic stem cells derived from C57BL/6 strain. Positive ES cells containing target vectors were identified by PCR and Southern bot analysis and microinjected into C57BL/6 blastocysts to generate chimeras. The resulting male chimeras were crossed to wild-type female C57BL/6 mice to generate heterozygous *Rock1*-floxed (*Rock1*$^{+/flox}$) mice. The F1 *Rock1*$^{+/flox}$ mice genotyped by PCR were crossed to *CAG-Flp* mice to remove the Neo cassette by the FLP-mediated recombination. We generated *Rock2*-floxed mice as previously described (1). αMHC (*Myh6*) promoter-driven Cre recombinase transgenic mice, which express Cre primarily in cardiomyocyte, were purchased from the Jackson Laboratory. To generate cardiac-specific ROCK1-deficient (*cROCK1*$^{-/-}$) mice and cardiac-specific ROCK2-deficient (*cROCK2*$^{-/-}$) mice, *Rock1*$^{flox/flox}$ mice and *Rock2*$^{flox/flox}$ mice were crossed with *Myh6-cre*$^{+/-}$ mice. The offspring were intercrossed. The resulting offspring, *Rock1*$^{flox/flox}$/*Myh6-cre*$^{+/-}$ mice (*cROCK1*$^{-/-}$ mice), *Rock2*$^{flox/flox}$/*Myh6-cre*$^{+/-}$ mice (*cROCK2*$^{-/-}$ mice) and their littermates were used for experiments. Animals were housed under a 12-h light and 12-h dark regimen and placed on a normal chow diet. The genotype of mice was confirmed by polymerase chain reaction (PCR) amplification using primers specific for the *Rock1*-floxed gene (5′-AAATGATTCCAGTTGCCCCTTGGATATTC-3′, 5′-TAAATTTAGACACAAACAATTCTGTAG-3′), *Rock2*-floxed gene (5′-TAAGACCTAGAGCACAGTC-3′, 5′-GGATTTGTTGGCACATCACTGAGTACC-3′) and *Myh6-cre* transgene (5′-GTTCGCAAGAACCTGATGGACA-3′, 5′-CTAGAGCCCTGTTTTGCACGTTC-3′).

Animal Experiments

All animal experiments were conducted in accordance with the protocols approved by the Tohoku University Animal Care and Use Committee (No. 2017-Kodo-004). Pressure overload-induced heart failure models were used to assess the roles of ROCK1 and ROCK2 on heart failure development in mice. Body weight between 23 and 27 g male cardiac-specific ROCK1-

deficient (*cROCK1*$^{-/-}$) mice, cardiac-specific ROCK2-deficient (*cROCK2*$^{-/-}$) mice and their littermate controls on a normal chow diet were exposed to pressure overload by transverse aortic constriction (TAC). TAC procedures were performed as we previously reported (2-4). Briefly, the animals were anesthetized with isoflurane and maintained body temperature. The transverse aorta was banded with a 6-0 suture, tied tight against a 25-gauge needle or a 27-gauge needle, which was removed quickly. Sham operated mice underwent the same procedure but without tying the transverse aorta. Mice with transverse aortic velocity above 4 m/s assessed by echocardiography were enrolled for the present study. The assessment of heart failure and histology were performed at 4 weeks after the operation. To determine the effect of ROCK1 and ROCK2 deficiency on pressure overload-induced heart failure, we performed cardiac echocardiography and weight measurements. All the operations and analyses were performed in a blinded manner with regard to the genotype of mice.

Blood Pressure, Echocardiography and Cardiac Catheterization

Blood pressure at baseline was measured by the tail-cuff system (Muromachi Kikai Co, Ltd, MK-2000ST NP-NIBP Monitor, Tokyo, Japan) without anesthesia. Echocardiography was performed using the Vevo 2100 (Visualsonics, Toronto, Canada) under inhalation of isoflurane (0.5-1.0% v/v). Echocardiography was performed to measure LV dimensions and systolic functions at the level of papillary muscles in M-mode tracings as previously described (3). In addition, Doppler signals of mitral inflow and myocardial tissue movement at the level of the mitral annulus were acquired from tilted parasternal long axis views to calculate E/A and E/e' as previously described (5). Cardiac catheterization was performed using a 1.2-F pressure catheter (SciSense Inc., Ontario, Canada) under inhalation of isoflurane (0.5-1.5 % v/v) as previously described (1, 6). For right heart catheterization, a 1.2-F pressure catheter was inserted into the right jugular vein and was advanced into the RV to measure pressure. For left heart catheterization, the catheter was inserted into the LV via apical approach after the mice were intubated and received ventilation. All data were analyzed using the PowerLab data acquisition system (AD Instruments) and averaged over 10 sequential beats.

Exercise Testing

Mice were tested for maximal speed and walking distance using a 5-lane rodent treadmill system (MK-680C, Muromachi Kikai, Japan). After an acclimation period during which mice were running at low speed (10 m/min), exercise testing was performed by having mice run at progressively increasing speeds (speed steps of 4 m/min every 3 minutes). Maximal speed and

running distance were determined when the mouse left the treadmill and remained on a shock pad for at least 5 sec.

Histology

After echocardiographic measurements, animals were anesthetized with isoflurane (2.0%). For morphological analysis, mice were perfused with cold phosphate-buffered saline (PBS) and perfusion-fixed with 10% phosphate-buffered formalin at physiological pressure for 5 min. The whole heart and lungs were harvested, fixed for 24 hours, embedded in paraffin and cross sections (5 μm) were prepared. Paraffin sections were stained with hematoxylin-eosin (HE) and Elastica-Masson (for analysis of the myocardial fibrosis area) or used for immunostaining. Antibody used was as follows; α-smooth muscle actin (αSMA, Sigma-Aldrich, 400:1). Pulmonary arteries adjacent to an airway distal to the respiratory bronchiole were evaluated as previously reported (7). Briefly, arteries were considered fully muscularized when they had a distinct double elastic lamina visible throughout the diameter of the vessel cross section. The arteries were considered partially muscularized when they had a distinct double elastic lamina visible for at least half the diameter. The percentage of vessels with double elastic lamina was calculated as the number of muscularized vessels per total number of vessels counted. In each section, a total of 60–80 vessels were examined by use of a computer-assisted imaging system (BX51, Olympus, Tokyo, Japan). This analysis was performed for the small vessels with external diameters of 20–70 μm. Cardiomyocyte cross-sectional area (CSA) was obtained by tracing the outlines of 100-200 cardiomyocytes with a clear nucleus image from the LV using HE stained sections. The fibrosis area of the myocardium was determined using EM stained sections in free wall area of the LV. These analyses were also performed by use of a computer-assisted imaging system (BX51, Olympus) and Image J Software (NIH, Bethesda, MD, USA).

Dihydroethidium Staining

The whole heart was harvested, embedded in OCT (Tissue-Tek; Miles Ink., Elkhart, Illinois, USA), snap-frozen, and cross-sections (10 μm) were prepared. Dihydroethidium (DHE), an oxidant fluorescent dye, was used to detect myocardial production of ROS as previously described (3, 4). Briefly, transverse sections were cut with a cryostat and placed on MAS-coated glass-slides (Matsunami Glass, Osaka, Japan). Then, the glass slides were incubated at 37°C for 30 min with DHE solution in PBS (2 μmol/L) in the shade. After washing with PBS, DHE red fluorescence (585nm) images were obtained using a confocal microscopy (Zeiss, LSM780).

Immunofluorescence staining

For immunofluorescence staining, mice were anesthetized with isoflurane and perfused with cold PBS and fixed by 4% phosphate-buffered paraformaldehyde, which were embedded in OCT. For immunostaining, we used the following primary antibodies; ROCK1 (200:1, BD Biosciences, 611136), ROCK2 (200:1, BD Biosciences, 610623), basigin (Bsg, 400:1, R&D systems, AF772), cyclophilin A (CyPA, 1000:1, Enzo Life Sciences, BML-SA296), periostin (400:1, abcam, ab14041), CD45 (400:1, BD Biosciences, 550539), COX IV (200:1, abcam, ab16056), and α-actinin (200:1, abcam, ab9465).

Matrix Metalloproteinase (MMP) Activity

For *in situ* zymography, freshly cut frozen heart sections (10 μm) were incubated with a fluorogenic gelatin substrate (DQ gelatin, Molecular Probes) dissolved to 25μg/mL in zymography buffer (50 mmol/L Tris-HCL pH7.4 and 5 mmol/L $CaCl_2$) according to the manufacturer's protocol (8). Proteolytic activity was detected as green fluorescence (530 nm) by confocal microscopy (Zeiss, LSM780).

MitoSOX Staining

Fresh frozen heart sections (10 μm) were incubated with 5μM MitoSOX Red (Thermo Fisher Scientific) in Hank's balanced salt solution containing 1mM $CaCl_2$ and 1mM $MgSO_4$ at 37℃ for 15 minutes. MitoSOX Red fluorescence images were acquired with a confocal microscopy (Zeiss, LSM780).

Measurements of Force and Intracellular Ca^{2+}

Trabeculae (length: 952 ± 21 μm; width: 121 ± 15 μm; thickness: 64 ± 3 μm in a slack condition) were dissected from the right ventricles of mouse hearts. Force was measured using a silicon strain gauge (model AE-801, SenSoNor, Horten, Norway). Intracellular Ca^{2+} was measured using microinjected fura-2 and a photomultiplier tube (PMT; E1341 with a C1556 socket, Hamamatsu, Japan). Trabeculae were electrically stimulated at 0.5 Hz with parallel platinum electrodes in a bath at 22℃.

Isolation of Neonatal Rat Cardiomyocytes

The hearts from neonatal Wistar rats (Japan SLC, Shizuoka, Japan) were minced and dissociated with collagenase type II (Worthington, NJ, USA). Then, cells were incubated on 10 cm dishes for 30 min at 37°C in 5% CO_2 incubator. To obtain neonatal rat cardiomyocytes (NRCMs),

non-attached viable cells in supernatant were collected and supplemented with 10 μM cytosine β-d-arabinofuranoside (Sigma-Aldrich, Tokyo, Japan) to prevent growth of non-myocytes(9). NRCMs were transfected with ROCK1 siRNA (10 nmol/l), ROCK2 siRNA (10 nmol/L) or control siRNA (10 nmol/L) (QIAGEN, Germany) for 72 hours to evaluate gene expressions. To examine the cellular effects of mechanical stress, NRCMs were subjected to cyclic stretch with 20% elongation at 1Hz for up to 24 hours using Strex system (Strex, Osaka, Japan) (10, 11). After the stimulus, total cell lysates were collected. Briefly, NRCMs were washed with cold PBS and harvested on ice in cell lysis buffer (#9803, Cell Signaling, MA, USA) with proteinase inhibitor cocktail (P8340, Sigma).

Seahorse Analyses

NRCMs (60,000-70,000 cells per well) were plated in 24-well Seahorse XFe24 cell culture microplates and were transfected with ROCK1 siRNA, ROCK2 siRNA, or control siRNA at 37ºC for 72 hours. After substituting growth media with assay media (XF modified DMEM supplemented with 5mM glucose and 1mM sodium pyruvate), cells were incubated in a CO_2-free incubator for equilibration prior to analyses. Oxygen consumption and extracellular acidification rates were measured using a Seahorse XFe24 Extracellular Flux Analyzer (Seahorse Bioscience/Agilent Technologies, North Billerica, MA). For mitochondrial flux, four cycles of baseline measurements were performed, followed by four 6-minute cycles each after the addition of 0.7 μM oligomycin (inhibitor of ATP synthase), 0.75 μM FCCP (proton ionophore), and 0.5 μM antimycin A plus rotenone (mitochondrial complex III and complex I inhibitors, respectively).

Western Blot Analysis

An equal amount of protein samples was loaded on SDS-PAGE gel and transferred to PVDF membranes (GE Healthcare, UK), and blocked for 1 hour at room temperature in 5 % BSA in Tris-Buffered Saline with Tween 20 (TBST). The primary antibodies used were as follows; ROCK1 (1000:1, Cell Signaling, #4035), ROCK2 (1000:1, BD Biosciences, 610624), RhoA (1000:1, Cell Signaling, #2117), GAPDH (1000:1, Cell Signaling, #2118), β-actin (1000:1, abcam, ab6276), phosphorylated-MYPT (1000:1, Millipore, ABS45), total-MYPT (1000:1, BD Biosciences, 612165), phosphorylated-Troponin I (1000:1, Cell Signaling, #4004), total-Troponin I (1000:1, Cell Signaling, #4004), phosphorylated-Phospholamban (Ser16) (1000:1, Santa Cruz, sc-12963-R), phosphorylated-Phospholamban (Thr17) (1000:1, Santa Cruz, sc-17024-R), total-Phospholamban (5000:1, Badrilla, A010-14), Drp1 (1000:1, BD Biosciences, 611112),

phosphorylated-Drp1 (Ser616) (1000:1, Cell Signaling, #3455), phosphorylated-Drp1 (Ser637) (1000:1, Cell Signaling, #4867), CyPA (1000:1, Enzo, BML-SA296-0100) and Bsg (1000:1, R&D systems, AF772). The regions containing proteins were visualized by the enhanced chemiluminescence system (ECL Prime Western Blotting Detection Reagent, GE Healthcare, Buckinghamshire, UK). Densitometric analysis was performed by the Image J Software.

RNA Isolation and Real-time PCR

Isolation of total RNA from mouse heart tissues and NRCM were performed using the RNeasy Plus Mini Kit (Qiagen) according to the manufacturer's protocol. Total RNA was converted to cDNA using PrimeScript RT Master Mix (Takara). Primers for murine *Nppa* (Assay ID: Mm01255747_g1), *Nppb* (Assay ID: Mm01255770_g1), *Col1a1* (Assay ID: Mm00801666_g1), *Col3a1* (Assay ID: Mm01254476_m1), *Atp2a2* (Assay ID: Mm01201431_m1), *Pln* (Assay ID: Mm04206542_m1), *Ryr2* (Assay ID: Mm00465877_m1), *Slc8a1* (Assay ID: Mm01232254_m1), *Cybb* (Assay ID: Mm01287743_m1), *Nox4* (Assay ID: Mm00479246_m1), *Ncf1* (Assay ID: Mm00447921_m1), *Ppargc1a* (Assay ID: Mm01208835_m1), *Tfam* (Assay ID: Mm00447485_m1), *Cytb* (Assay ID: Mm04225271_g1), *Nd5 Nd6* (Assay ID: Mm04225315_s1), *Fis1* (Assay ID: Mm00481580_m1), *Mff* (Assay ID: Mm01273401_m1), *Pink1* (Assay ID: Mm00550827_m1), *Park2* (Assay ID: Mm00450187_m1), *Opa1* (Assay ID: Mm01349707_g1), *Mfn1* (Assay ID: Mm00612599_m1), *Mfn2* (Assay ID: Mm00500120_m1), *Gapdh* (Assay ID: Mm99999915_g1), and primers for rat *Ppia* (Assay ID: Rn00690933_m1), *Bsg* (Assay ID: Rn00680749_g1) and *Gapdh* (Assay ID: Rn01775763_g1) were purchased from Life Technologies (TaqMan assays, Applied Biosystems, US). Primers for rat *Rock1* (Primer Set ID: RA061446), *Rock2* (Primer Set ID: RA066811), *Cybb* (Primer Set ID: RA052264), *Nox4* (Primer Set ID: RA064409), *Ncf1* (Primer Set ID: RA061065) and *Gapdh* (Primer Set ID: RA015380) were purchased from Takara Bio Inc. (SYBR Green I assays, Shiga, Japan). After reverse transcription, quantitative real-time PCR on the CFX 96 Real-Time PCR Detection System (Bio-Rad) was performed using either SsoFast Probes Supermix (Bio-Rad) for TaqMan probes or SYBR® Premix Ex Taq™ II (Takara) for SYBR probes. The Ct value determined by CFX Manager Software (version2.0, Bio-Rad) for all samples was normalized to housekeeping gene *Gapdh* and the relative fold change was computed by the ΔΔCt method (3).

Microarray

Total RNA was extracted from the left ventricular free wall of *cROCK1*$^{-/-}$ mice, *cROCK2*$^{-/-}$ mice and their littermate controls and was quantified using NanoDrop 2000C (Thermo Fisher

Scientific). For microarray expression profiling, samples were processed using the Agilent SurePrint G3 Mouse GE 8x60K Microarray Kit (Agilent Technologies, Santa Clara, CA) according to the manufacturer's instructions. The statistical computing software R (version 3.3.2.) and samr (version 2.0) package of R were used for preprocessing and statistical analysis. Differentially expressed genes were considered significant at SAM *t*-test P values of < 0.05. Genes with significant changes were further subjected to pathway analysis using Ingenuity Pathway Analysis (IPA) (http://www.ingenuity.com) to identify gene sets representing specific biological processes or functions.

Transmission Electron Microscopy

The ultrastructure of mitochondria in the heart was visualized using transmission electron microscopy (TEM). For TEM assessment, hearts were perfused with cold PBS and were fixed in 2% paraformaldehyde and 2.5% glutaraldehyde, followed by fixation in 1% osmic acid and embedding in Epon. Ultrathin sections were made using Leica EM UC7 (Leica Microsystems, Wetzlar, Germany) and observed with a H-7600 transmission electron microscope (Hitachi High-Technologies Co., Tokyo, Japan).

High-throughput Screening

Libraries of drugs and bioactive compounds containing 3,336 unique compounds were available from the Drug Discovery Initiative (DDI), the University of Tokyo (http://www.ddi.u-tokyo.ac.jp/en/). Pulmonary artery smooth muscle cells (PASMCs) harvested from patients with pulmonary arterial hypertension (PAH-PASMCs) were used for the first (proliferation assay) and second (RT-PCR) screening and control PASMCs were used for counter assay (proliferation assay). We optimized screening conditions (cell number, time-course of plating cells, and adding stimulus) beforehand. PAH-PASMCs were grown in DMEM (10% FBS, 1% Penicillin/Streptomycin) up to 80% confluency. The cells were trypsinized and resuspended in complete medium. They were counted and 1,000 cells/45μL were plated in each well of a 384-well plate (781182, Cell culture microplate 384 well, Greiner Bio-One, Austria) using the Multidrop™ Combi (Thermo Scientific). They were then placed in the automated incubator at 37°C for 24 hours. Fifteen μL of the diluted compounds were added to columns 3-22 of every plate by the Biomek NXP (Beckman Coulter, Brea, CA) (compounds 5 μM, DMSO 0.5% final concentration). Dimethyl sulfoxide (DMSO, Wako, Osaka, Japan) in the same concentration (0.5%) was used as negative control. The plates were incubated for an additional 48 hours and 10 μL Cell Titer 96 AQueous One Solution Cell Proliferation Assay kit (Promega) was added to

each well and the plates were read after 2 hours of incubation in the SpectraMax Paradigm (Molecular Devices). Hits were determined as compounds that suppressed PAH-PASMCs proliferation by > 20% compared with control. The intra-plate and inter-plate variability in a pilot screen using 12 x 384 well plates showed a coefficient of variance of 5.9% and 4.0%, respectively.

Celastrol Treatment

Eight-week-old male C57BL/6 mice were subjected to TAC or sham operation and daily administered either celastrol (1 mg/kg/day) or vehicle via intraperitoneal injection. Celastrol was purchased from Tokyo Chemical Industry Co. and the dosage and treatment schedule were chosen according to the recent report (12). The assessment of heart failure was performed at 4 weeks after TAC. To determine the effect of celastrol on pressure overload-induced heart failure, we performed cardiac echocardiography, right heart catheterization, weight measurements.

Measurements of Plasma Levels of Cyclophilin A

The Ethical Review Board of Tohoku University approved the study protocol, and written informed consent was obtained from all patients (No. 2008-363). Patients with hypertension were regarded as being at risk if their blood pressure was ≥140/90 mmHg or if they had a history of antihypertensive drug use. Patients with diabetes mellitus were regarded as being at risk if their fasting glucose level was ≥126 mg/dL or if they had a history of hypoglycemic drug or insulin use. Patients with dyslipidemia were regarded as being at risk if their LDL cholesterol level was ≥140 mg/dL or their HDL cholesterol level was ≤40 mg/dL, or if they were taking a lipid-lowering drug. Fasting blood samples were collected for measurement of CyPA concentration from the antecubital vein in the supine position. Plasma samples were collected using EDTA and were centrifuged for 10 min at 2,500 g within 30 min of blood collection, and aliquots were stored at -80°C. Plasma CyPA levels were measured using an immunoassay based on the sandwich technique according to the manufacturer's protocol (Human Cyclophilin A ELISA Kit, CSB-E09920h, Cusabio).

CART Analysis

To identify the cut-off point of plasma CyPA levels that is able to classify heart failure patients for all-cause death, we have performed the classification and regression trees (CART) analysis. The CART analysis is an empirical, statistical technique based on recursive partitioning of the

data space to predict the response. The models were obtained by binary splitting of the data by the value of predictors, and the split variable and split-point were automatically selected from possible candidate predictor values to achieve the best fit. Then, one or both "child nodes" were split into two regions recursively, and the process continued until some stopping rule was applied. Finally, the result of this process is expressed as a binary decision tree (13).

Statistical Analyses

All results are shown as mean ± SEM. Comparisons of means between 2 groups were performed by unpaired Student's *t*-test or one-way analysis of variance (ANOVA) with interaction terms, followed by Tukey's HSD (honestly significant difference) for multiple comparisons. Comparisons of mean responses associated with the two main effects of the different genotypes and the severity of pulmonary vascular remodeling were performed by two-way ANOVA with interaction terms, followed by Tukey's HSD for multiple comparisons. Statistical significance was evaluated with JMP 12 (SAS Institute Inc, Cary, America) or R version 3.3.2 (http://www.R-project.org/). The ratio of fully muscularized vessels was analyzed by the Poisson regression with the offset equals to the sum of total vessels with multcomp 1.4-6 package or R. All reported p values are 2-tailed, with a p value of less than 0.05 indicating statistical significance.

Supplementary Table 1

Top 10 Significant Canonical Pathways in *cROCK1*$^{-/-}$ Hearts

No.	Top canonical pathways
1	RhoA signaling
2	Regulation of actin-based motility by Rho
3	Regulation of cellular mechanics by calpain protease
4	nNOS signaling in skeletal muscles cells
5	Calcium signaling
6	RhoGDI Signaling
7	Agrin interactions at neuromuscular junction
8	nNOS signaling in neurons
9	Oleate biosynthesis II (animals)
10	Agranulocyte adhesion and diapedesis

Supplementary Table 2

Top 10 Significant Canonical Pathways in *cROCK2*$^{-/-}$ Hearts

No.	Top canonical pathways
1	Glutamate receptor signaling
2	Tryptophan degradation X (mammalian, via Tryptamine)
3	Role of IL-17A in psoriasis
4	Cardiac β-adrenergic signaling
5	Fatty acid activation
6	Ephrin receptor signaling
7	cAMP-mediated signaling
8	Axonal guidance signaling
9	Serotonin receptor signaling
10	γ-linolenate biosynthesis II (animals)

Supplementary Table 3

Clinical backgrounds

	Control (*n*=25)	CHF without PH (*n*=72)	CHF with PH (*n*=54)
Clinical characteristics			
Age (years-old)	60.8±15.1	61.9±15.9	59.5±14.0
Male sex, %	48.0	58.7	46.8
BMI (kg/m^2)	24.2±2.7	22.8±3.7	23.1±5.3
Hypertension, %	64.0	39.7	38.3
Dyslipidemia, %	60.0	22.2	12.8
Diabetes mellitus, %	44.0	12.7	19.2
eGFR, ml/min per 1.73 m^2	70.0±15.4	58.5±20.2	49.6±24.8
BNP pg/ml	33.1±34.7	264.6±569.3	523.0±760.8
NYHA class, %			
I		33.9	8.7
II		51.6	52.2
III		11.3	37.0
IV		3.2	2.2
Medication			
Aldactone, %	0	30.2	46.8
ACE-I, %	16.0	42.9	46.8
ARB, %	28.0	30.2	34.0
β-blocker, %	12.0	42.9	63.8

Plus-minus values are average ± SD. BMI indicates body mass index; eGFR, estimated glomerular filtration rate; BNP, brain natriuretic peptide; NYHA, New York heart association; ACE-I, angiotensin-converting enzyme inhibitor; ARB, angiotensin-receptor blocker.

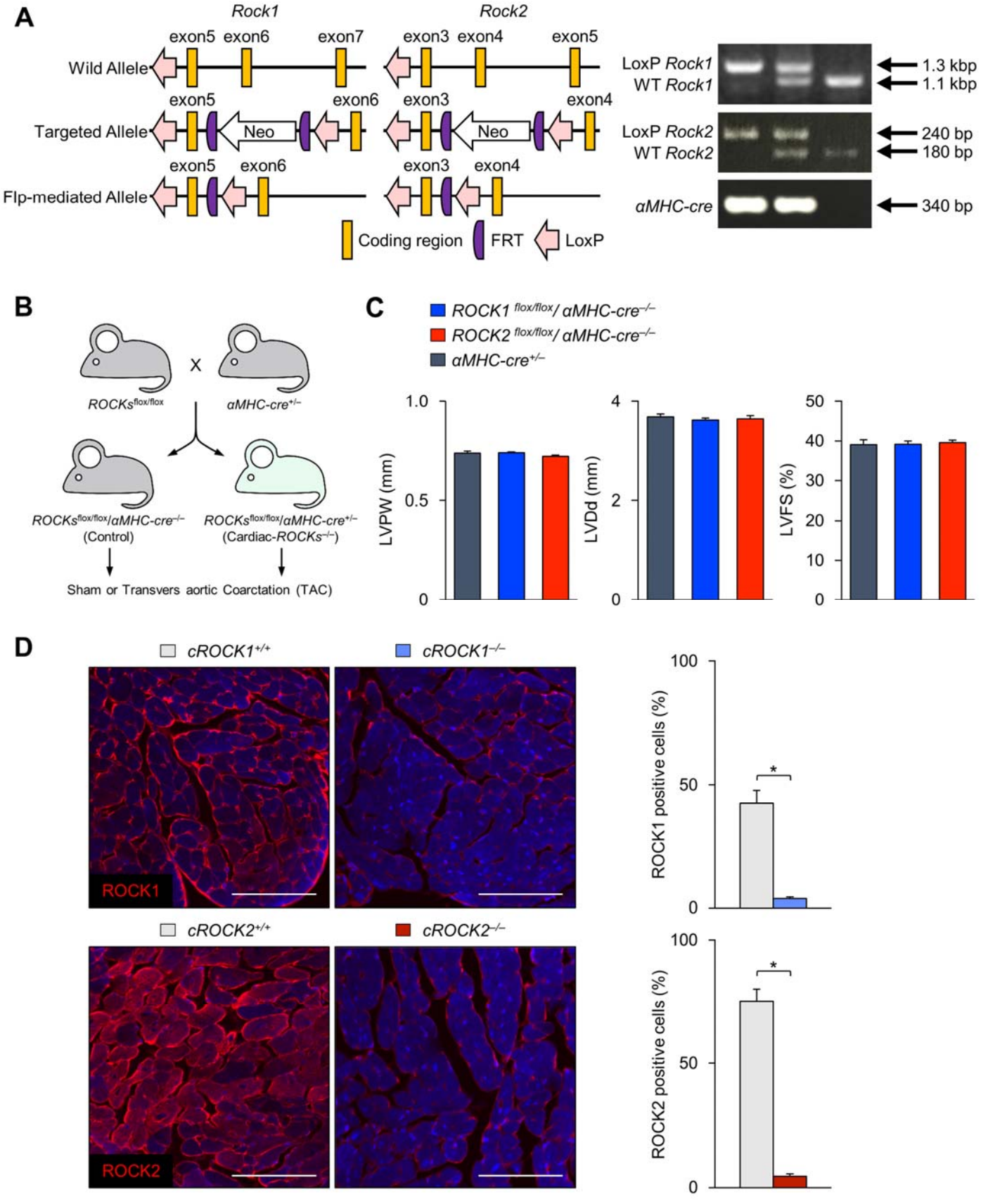
A
Rock1
Rock2
exon5 exon6 exon7
exon3 exon4 exon5
Wild Allele
exon5 exon6
exon3 exon4
Targeted Allele
Neo
Neo
exon5 exon6
exon3 exon4
Flp-mediated Allele
Coding region
FRT
LoxP
LoxP Rock1
WT Rock1
1.3 kbp
1.1 kbp
LoxP Rock2
WT Rock2
240 bp
180 bp
αMHC-cre
340 bp
B
X
ROCKs flox/flox
αMHC-cre+/–
ROCKs flox/flox/αMHC-cre–/–
(Control)
ROCKs flox/flox/αMHC-cre+/–
(Cardiac-ROCKs–/–)
Sham or Transvers aortic Coarctation (TAC)
C
ROCK1 flox/flox/ αMHC-cre–/–
ROCK2 flox/flox/ αMHC-cre–/–
αMHC-cre+/–
LVPW (mm)
1.0
0.5
0
LVDd (mm)
4
2
0
LVFS (%)
50
40
30
20
10
0
D
cROCK1+/+
cROCK1–/–
ROCK1
cROCK2+/+
cROCK2–/–
ROCK2
ROCK1 positive cells (%)
100
50
0
*
ROCK2 positive cells (%)
100
50
0
*

Figure S1. Generation of cardiac-specific ROCK1-deficient and ROCK2-deficient mice
(**A**) Illustration of wild-type *Rock1* and *Rock2* allele and conditional targeted allele (floxed allele). Genotyping by PCR on genomic DNA isolated from tail of *cROCK1*$^{-/-}$, *cROCK1*$^{+/-}$, *cROCK2*$^{-/-}$, *cROCK2*$^{+/-}$ and wild-type mice. (**B**) Schematic outline for generating cardiac-specific ROCKs knockout mice. (**C**) Quantitative analysis of the echocardiographic parameters of cardiac structure and function in *cROCK1*$^{+/+}$ (*ROCK1* $^{flox/flox}$*/ aMHC-cre*$^{-/-}$), *cROCK2*$^{+/+}$ (*ROCK2* $^{flox/flox}$*/ aMHC-cre*$^{-/-}$), and *aMHC-cre*$^{+/-}$ mice (*n*=3 each) at baseline. (**D**) Representative photomicrographs of fluorescent immunostaining showing the localization of ROCK1 and ROCK2 expressions (red, Alexa flour 546) in the left ventricle at baseline and mean data for the % of cells positive for ROCK1 and ROCK2. Scale bars, 100μm. Data represent the mean ± s.e.m. Comparisons of parameters were performed with the unpaired Student's *t*-test.

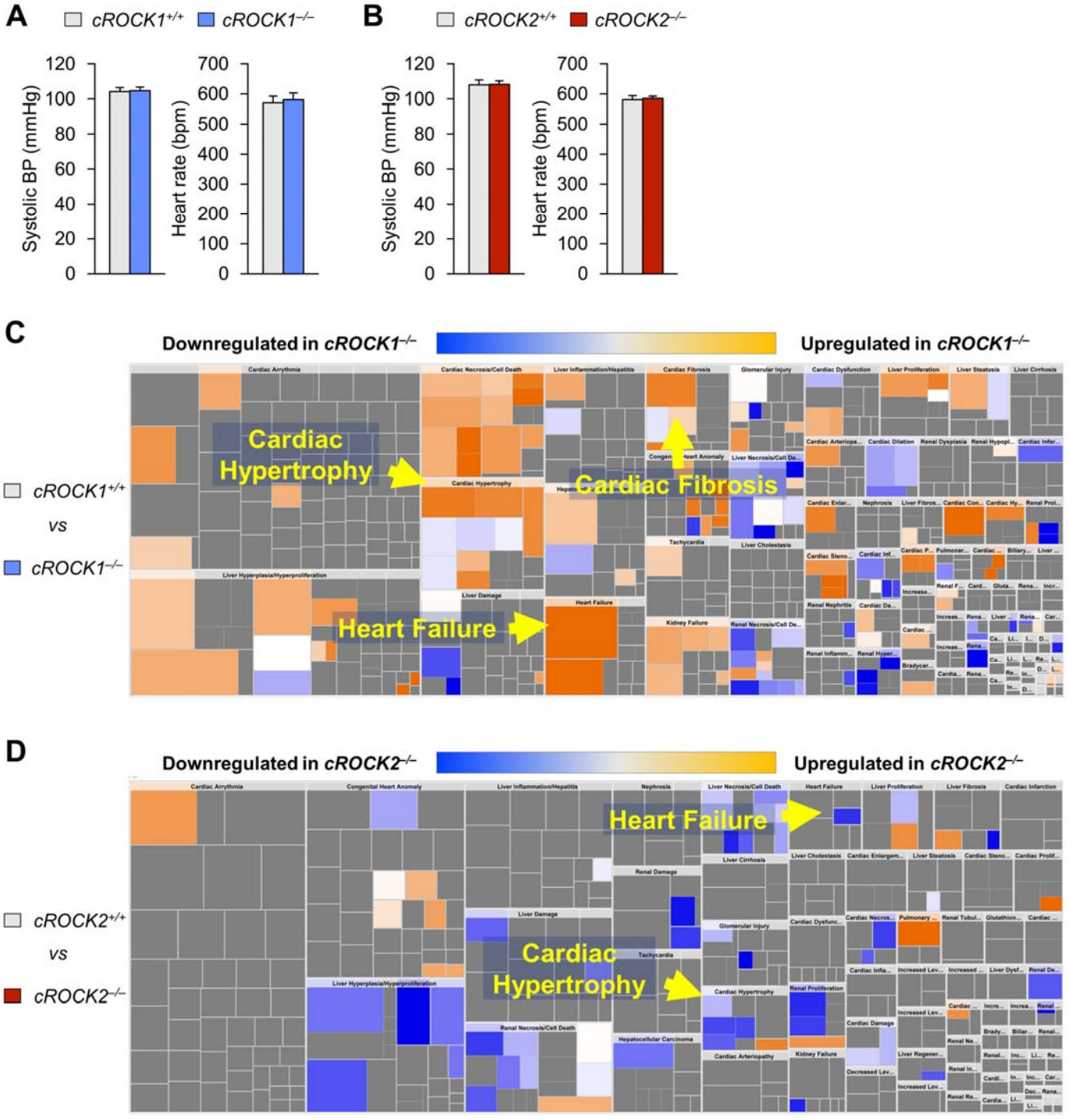
A
cROCK1+/+
cROCK1−/−
Systolic BP (mmHg)
Heart rate (bpm)
B
cROCK2+/+
cROCK2−/−
Systolic BP (mmHg)
Heart rate (bpm)
C
Downregulated in cROCK1−/−
Upregulated in cROCK1−/−
cROCK1+/+
vs
cROCK1−/−
Cardiac Hypertrophy
Cardiac Fibrosis
Heart Failure
D
Downregulated in cROCK2−/−
Upregulated in cROCK2−/−
cROCK2+/+
vs
cROCK2−/−
Heart Failure
Cardiac Hypertrophy

Figure S2. Baseline characteristics of cardiac-specific ROCK1-deficient and ROCK2-deficient mice

(**A**) Heart rate and blood pressure measured by tail-cuff method in *cROCK1*$^{+/+}$ and *cROCK1*$^{-/-}$ mice (*n*=6 each). (**B**) Heart rate and blood pressure measured by tail-cuff method in *cROCK2*$^{+/+}$ and *cROCK2*$^{-/-}$ mice (*n*=6 each). (**C,D**) Heat map analysis of gene microarray analyses by Ingenuity Pathway Analysis software. Data represent the mean ± s.e.m. Comparisons of parameters were performed with the unpaired Student's *t*-test.

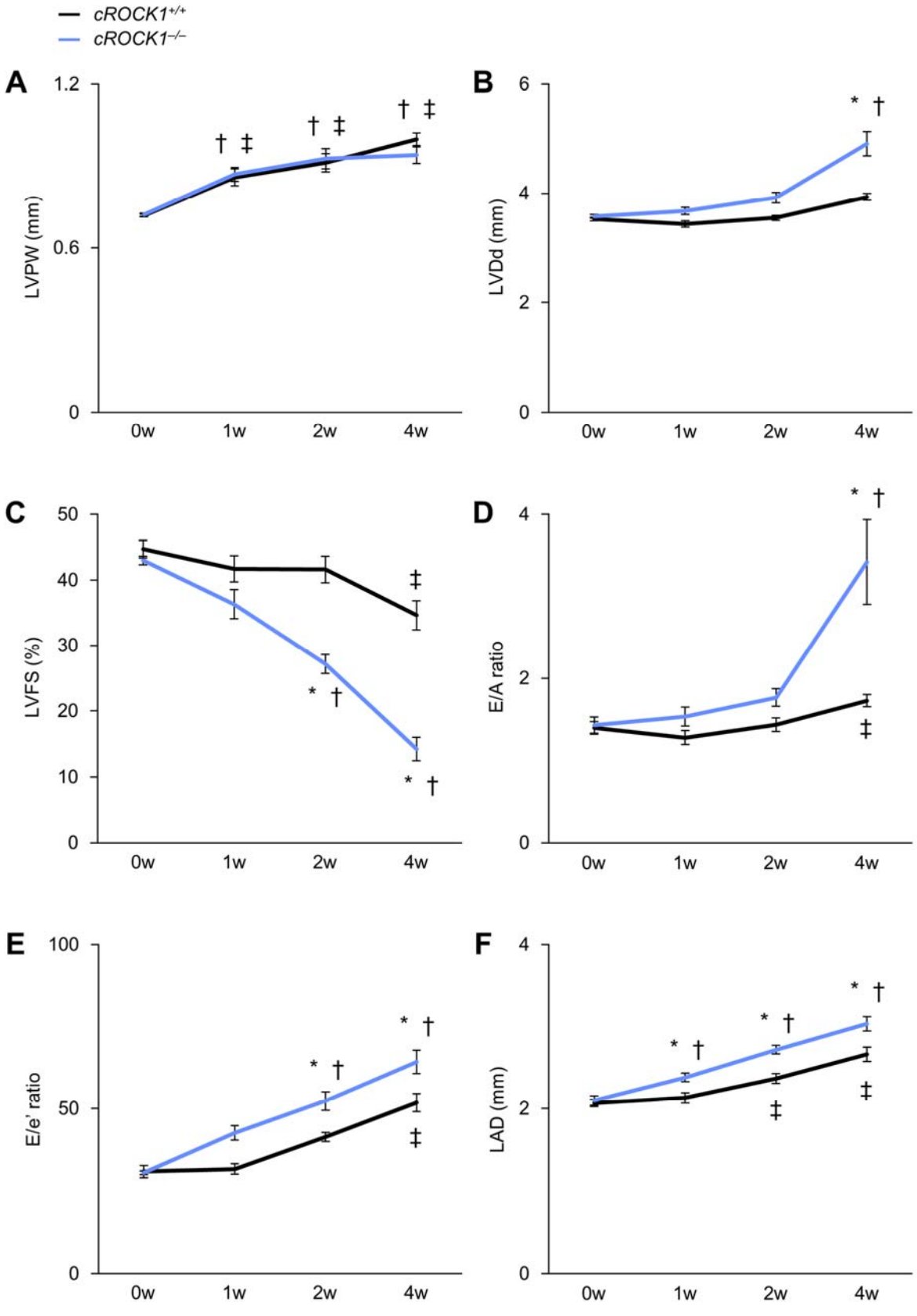
cROCK1+/+
cROCK1−/−
A
LVPW (mm)
1.2
0.6
0
B
LVDd (mm)
6
4
2
0
C
LVFS (%)
50
40
30
20
10
0
D
E/A ratio
4
2
0
E
E/e' ratio
100
50
0
F
LAD (mm)
4
2
0
0w
1w
2w
4w

Figure S3. Time course analysis of cardiac structure and function in *cROCK1*$^{+/+}$ and *cROCK1*$^{-/-}$ mice after TAC

(**A**~**F**) Time course analysis of left ventricular (LV) posterior wall thickness (LVPW), LV internal diameter at end-diastole (LVDd), LV fractional shortening (LVFS), E/A ratio, E/e' ratio and left atrial diameter (LAD) in *cROCK1*$^{+/+}$ and *cROCK1*$^{-/-}$ mice after TAC (*n*=8 each). Data represent the mean ± s.e.m. **P*<0.05 vs. *cROCK1*$^{+/+}$ at the same week after TAC. †*P*<0.05 vs. *cROCK1*$^{-/-}$ at 0 week. ‡*P*<0.05 vs. *cROCK1*$^{+/+}$ at 0 week. Comparisons of parameters were performed with unpaired Student's *t*-test or two-way ANOVA followed by unpaired Student's *t*-test.

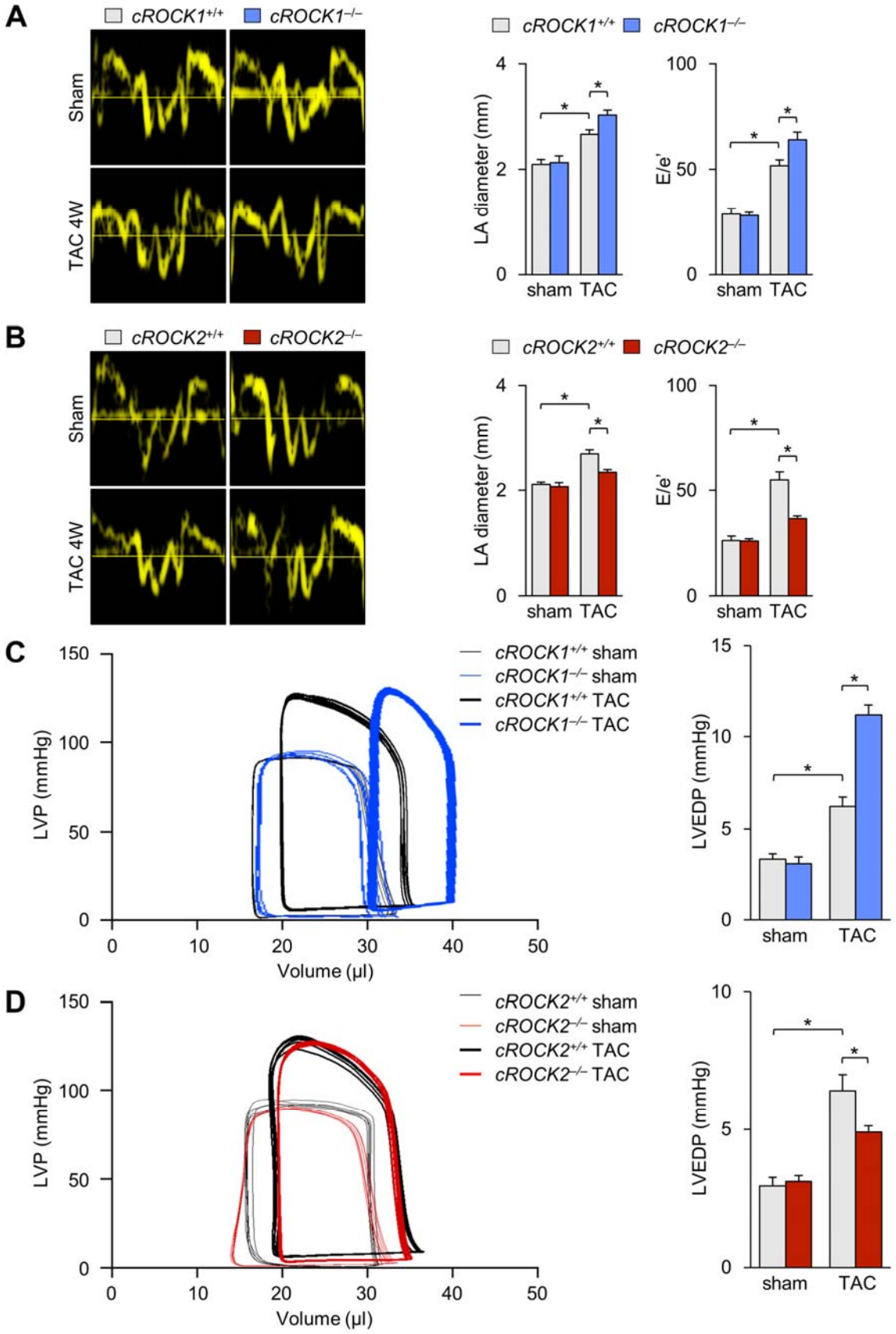
A
cROCK1+/+
cROCK1−/−
Sham
TAC 4W
LA diameter (mm)
E/e'
sham
TAC
B
cROCK2+/+
cROCK2−/−
C
cROCK1+/+ sham
cROCK1−/− sham
cROCK1+/+ TAC
cROCK1−/− TAC
LVP (mmHg)
Volume (μl)
LVEDP (mmHg)
D
cROCK2+/+ sham
cROCK2−/− sham
cROCK2+/+ TAC
cROCK2−/− TAC

Figure S4. Assessment of filling pressures after TAC

(**A**) Representative tissue Doppler images of mitral annulus in *cROCK1*$^{+/+}$ and *cROCK1*$^{-/-}$ mice at 4 weeks after transverse aortic constriction (TAC) or sham operation and quantitative analysis of left atrial (LA) diameter and E/e' in *cROCK1*$^{+/+}$ and *cROCK1*$^{-/-}$ mice at 4 weeks after TAC (n=10 each) or sham operation (n=5 each). (**B**) Representative tissue Doppler images of mitral annulus in *cROCK2*$^{+/+}$ and *cROCK2*$^{-/-}$ mice at 4 weeks after TAC or sham operation and quantitative analysis of LA diameter and E/e' in *cROCK2*$^{+/+}$ and *cROCK2*$^{-/-}$ mice at 4 weeks after TAC (n=10 each) or sham operation (n=5 each). (**C**) Representative left ventricular (LV) pressure-volume loops in *cROCK1*$^{+/+}$ and *cROCK1*$^{-/-}$ mice at 4 weeks after TAC or sham operation and quantitative analysis of left ventricular end-diastolic pressure (LVEDP) in *cROCK1*$^{+/+}$ and *cROCK1*$^{-/-}$ mice at 4 weeks after TAC (n=8 each) or sham operation (n=5 each). (**D**) Representative LV pressure-volume loops in *cROCK2*$^{+/+}$ and *cROCK2*$^{-/-}$ mice at 4 weeks after TAC or sham operation and quantitative analysis of LVEDP in *cROCK2*$^{+/+}$ and *cROCK2*$^{-/-}$ mice at 4 weeks after TAC (n=9 each) or sham operation (n=5 each). Data represent the mean ± s.e.m. *P<0.05. Comparisons of parameters were performed with two-way ANOVA followed by Tukey's HSD test for multiple comparisons.

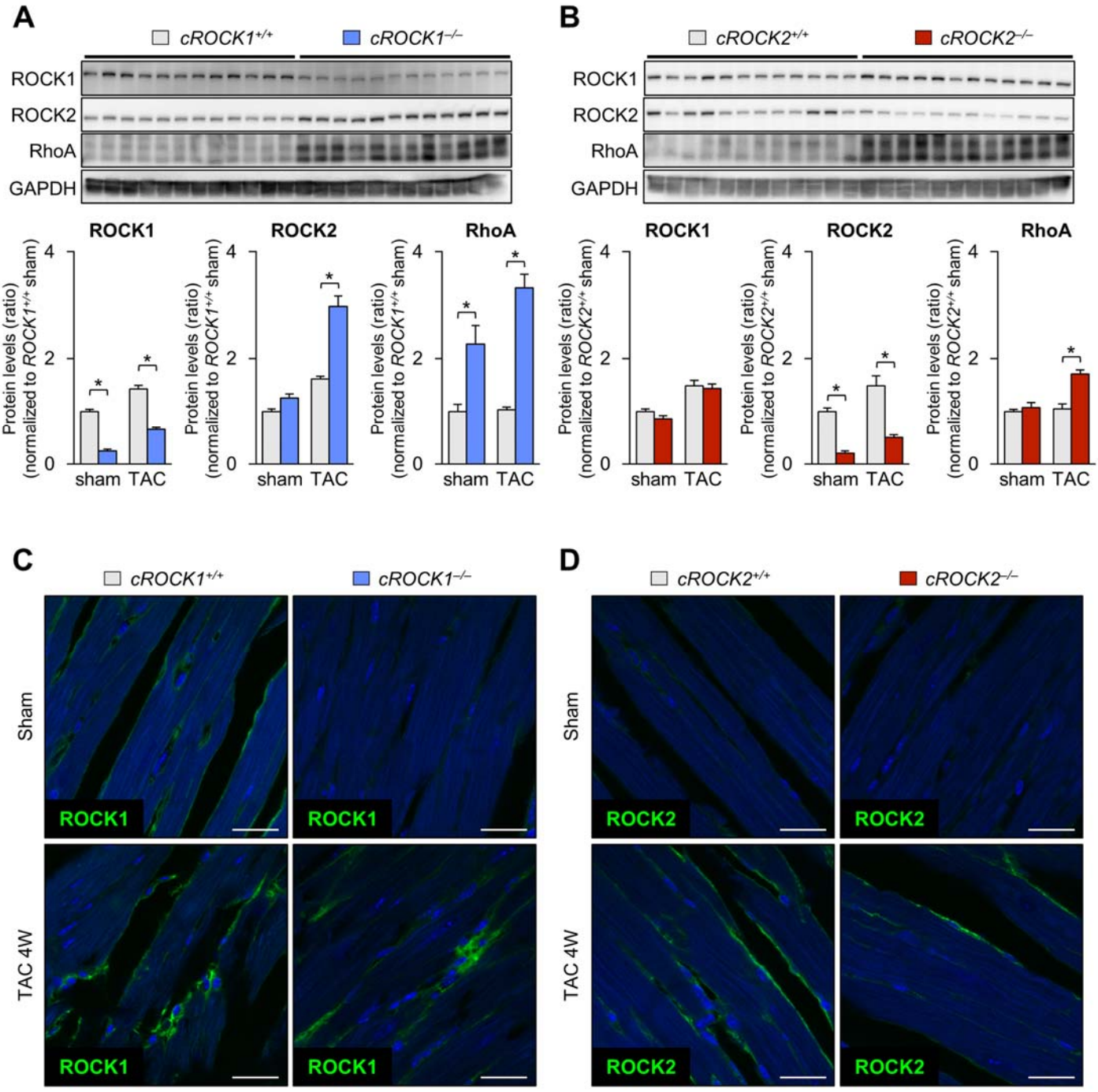
A
cROCK1+/+
cROCK1−/−
ROCK1
ROCK2
RhoA
GAPDH
ROCK1
ROCK2
RhoA
Protein levels (ratio) (normalized to ROCK1+/+ sham)
sham TAC
B
cROCK2+/+
cROCK2−/−
ROCK1
ROCK2
RhoA
GAPDH
ROCK1
ROCK2
RhoA
Protein levels (ratio) (normalized to ROCK2+/+ sham)
sham TAC
C
cROCK1+/+
cROCK1−/−
Sham
TAC 4W
ROCK1
D
cROCK2+/+
cROCK2−/−
Sham
TAC 4W
ROCK2

Figure S5. Rho-kinase and RhoA expressions in LV induced by pressure overload
(**A**) Representative Western blot and quantification of ROCK1, ROCK2, RhoA and GAPDH expressions in *cROCK1*$^{+/+}$ and *cROCK1*$^{-/-}$ hearts at 4 weeks after transverse aortic constriction (TAC, *n*=12 each) or sham operation (*n*=5 each). (**B**) Representative Western blot and quantification of ROCK1, ROCK2, RhoA and GAPDH expressions in *cROCK2*$^{+/+}$ and *cROCK2*$^{-/-}$ hearts at 4 weeks after TAC (*n*=12 each) or sham operation (*n*=5 each). (**C**) Representative photomicrographs of fluorescent immunostaining showing the localization of ROCK1 (green, Alexa flour 488) in the left ventricle in *cROCK1*$^{+/+}$ and *cROCK1*$^{-/-}$ mice at 4 weeks after TAC or sham operation. (**D**) Representative photomicrographs of fluorescent immunostaining showing the localization of ROCK2 (green, Alexa flour 488) in the left ventricle in *cROCK2*$^{+/+}$ and *cROCK2*$^{-/-}$ mice at 4 weeks after TAC or sham operation. Scale bars, 25μm. Data represent the mean ± s.e.m. **P*<0.05. Comparisons of parameters were performed with two-way ANOVA followed by Tukey's HSD test for multiple comparisons.

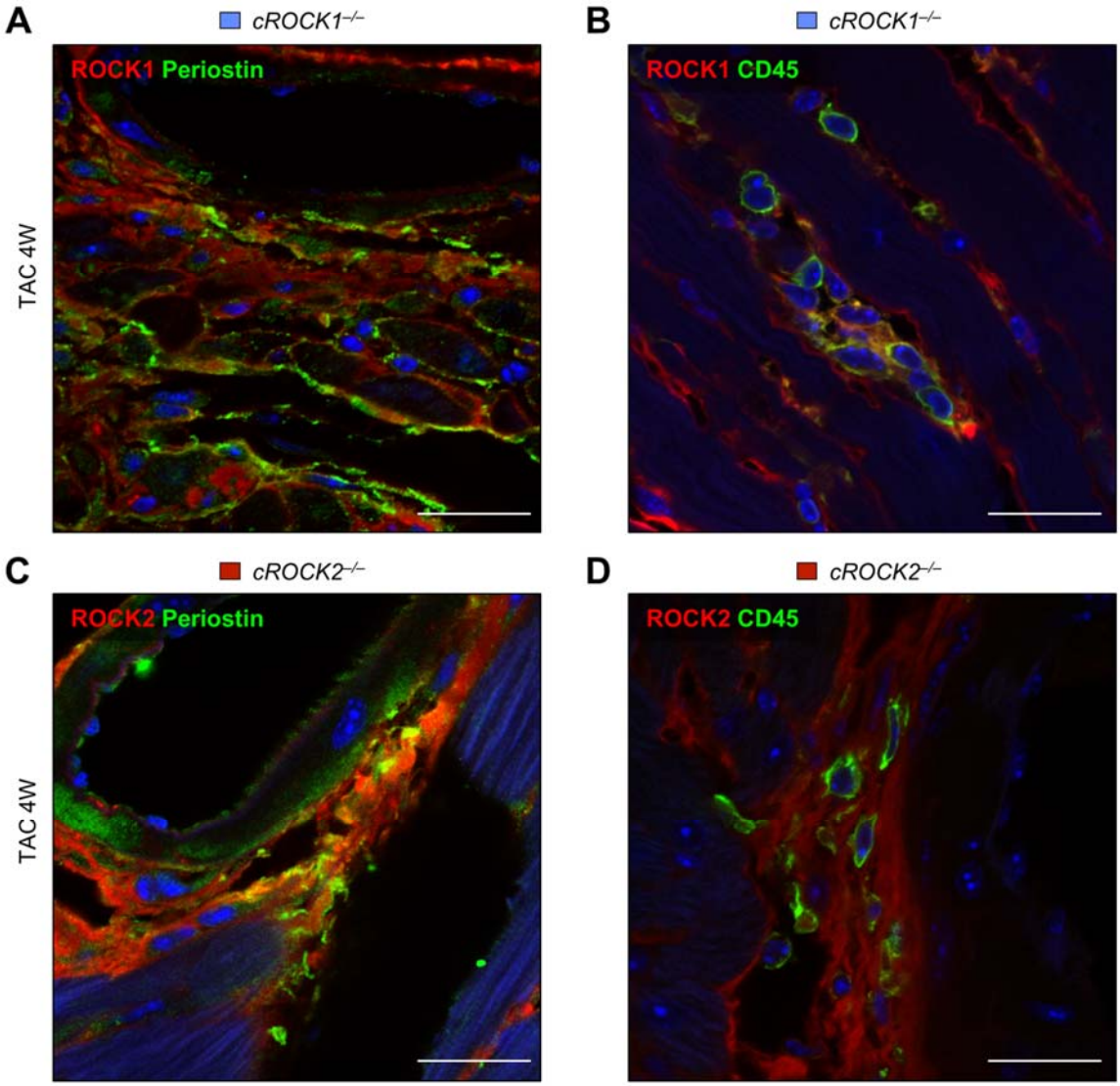

Figure S6. ROCK1/ROCK2 expression in perivascular inflammatory cells and cardiac fibroblasts after pressure overload

(**A**) Representative immunostaining showing the localization of ROCK1 (red, Alexa flour 546), periostin (green, Alexa flour 488), and DAPI in the left ventricle (LV) in *cROCK1*$^{-/-}$ mice at 4 weeks after transverse aortic constriction (TAC). (**B**) Representative immunostaining showing the localization of ROCK1 (red, Alexa flour 546), CD45 (green, Alexa flour 488), and DAPI in the LV in *cROCK1*$^{-/-}$ mice at 4 weeks after TAC. (**C**) Representative immunostaining showing the localization of ROCK2 (red, Alexa flour 546), periostin (green, Alexa flour 488), and DAPI in the LV in *cROCK2*$^{-/-}$ mice at 4 weeks after TAC. (**D**) Representative immunostaining showing the localization of ROCK2 (red, Alexa flour 546), CD45 (green, Alexa flour 488), and DAPI in the LV in *cROCK2*$^{-/-}$ mice at 4 weeks after TAC. Scale bars, 25μm.

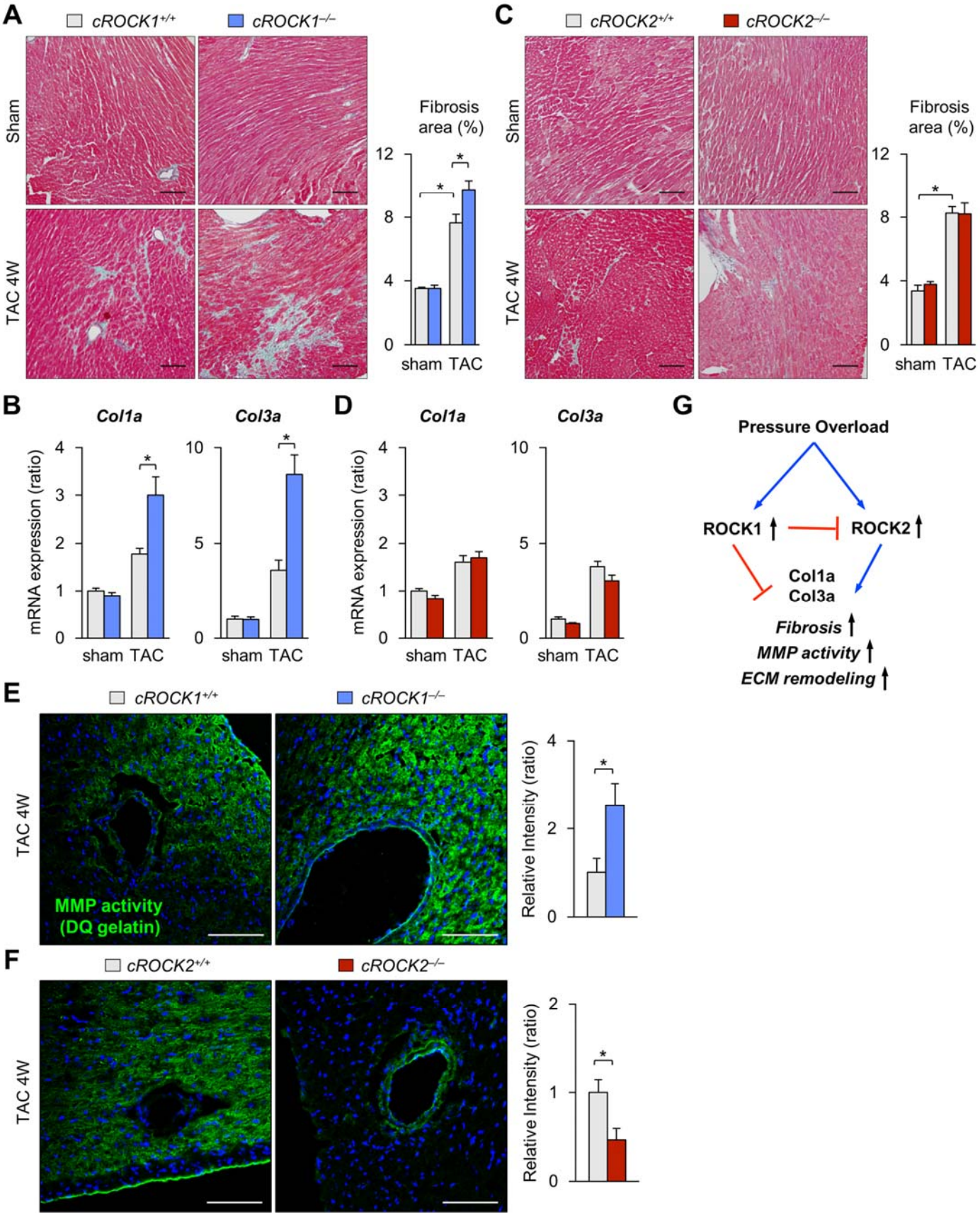
A
cROCK1+/+
cROCK1−/−
Sham
TAC 4W
Fibrosis area (%)
12
8
4
0
sham TAC
C
cROCK2+/+
cROCK2−/−
Sham
TAC 4W
Fibrosis area (%)
12
8
4
0
sham TAC
B
Col1a
Col3a
mRNA expression (ratio)
4
3
2
1
0
10
5
0
sham TAC
D
Col1a
Col3a
mRNA expression (ratio)
4
3
2
1
0
10
5
0
sham TAC
G
Pressure Overload
ROCK1
ROCK2
Col1a
Col3a
Fibrosis
MMP activity
ECM remodeling
E
cROCK1+/+
cROCK1−/−
TAC 4W
MMP activity
(DQ gelatin)
Relative Intensity (ratio)
4
2
0
F
cROCK2+/+
cROCK2−/−
TAC 4W
Relative Intensity (ratio)
2
1
0

Figure S7. Myocardial ROCK1 deletion enhances pressure overload-induced cardiac fibrosis.

(**A**) Left, representative photomicrographs of Elastica-Masson (EM) staining of *cROCK1*$^{+/+}$ and *cROCK1*$^{-/-}$ hearts 4 weeks after transverse aortic constriction (TAC) or sham operation. Right, quantitative analysis of interstitial fibrotic area in *cROCK1*$^{+/+}$ and *cROCK1*$^{-/-}$ mice at 4 weeks after TAC (*n*=10 each) or sham operation (*n*=5 each). Scale bars, 100 μm (**B**) Relative mRNA expressions of fibrotic markers, such as collagen 1a (*Col1a*) and collagen 3a (*Col3a*), in *cROCK1*$^{+/+}$ and *cROCK1*$^{-/-}$ hearts at 4 weeks after TAC (*n*=12 each) or sham operation (*n*=5 each). (**C**) Left, representative photomicrographs of EM staining of *cROCK2*$^{+/+}$ and *cROCK2*$^{-/-}$ hearts 4 weeks after TAC or sham operation. Right, quantitative analysis of interstitial fibrotic area in *cROCK2*$^{+/+}$ and *cROCK2*$^{-/-}$ hearts at 4 weeks after TAC (*n*=10 each) or sham operation (*n*=5 each). Scale bars, 100 μm. (**D**) Relative mRNA expressions of *Col1a* and *Col3a* in *cROCK2*$^{+/+}$ and *cROCK2*$^{-/-}$ hearts at 4 weeks after TAC (*n*=12 each) or sham operation (*n*=5 each). (**E**) Representative pictures of *in situ* zymography (DQ gelatin) for matrix metaroproteinase (MMP) activities and its relative intensity in the left ventricles of *cROCK1*$^{+/+}$ and *cROCK1*$^{-/-}$ mice after TAC (*n*=8 each). Scale bars, 100μm. (**F**) Representative pictures of DQ gelatin for MMP activities and its relative intensity in the left ventricles of *cROCK2*$^{+/+}$ and *cROCK2*$^{-/-}$ mice after TAC (*n*=8 each). Scale bars, 100μm. (**G**) Schematic representation of the different roles of ROCK1 and ROCK2 in cardiac fibrosis and extracellular matrix (ECM) remodeling. Data represent the mean ± s.e.m. **P*<0.05. Comparisons of parameters were performed with the unpaired Student's *t*-test or two-way ANOVA followed by Tukey's HSD test for multiple comparisons.

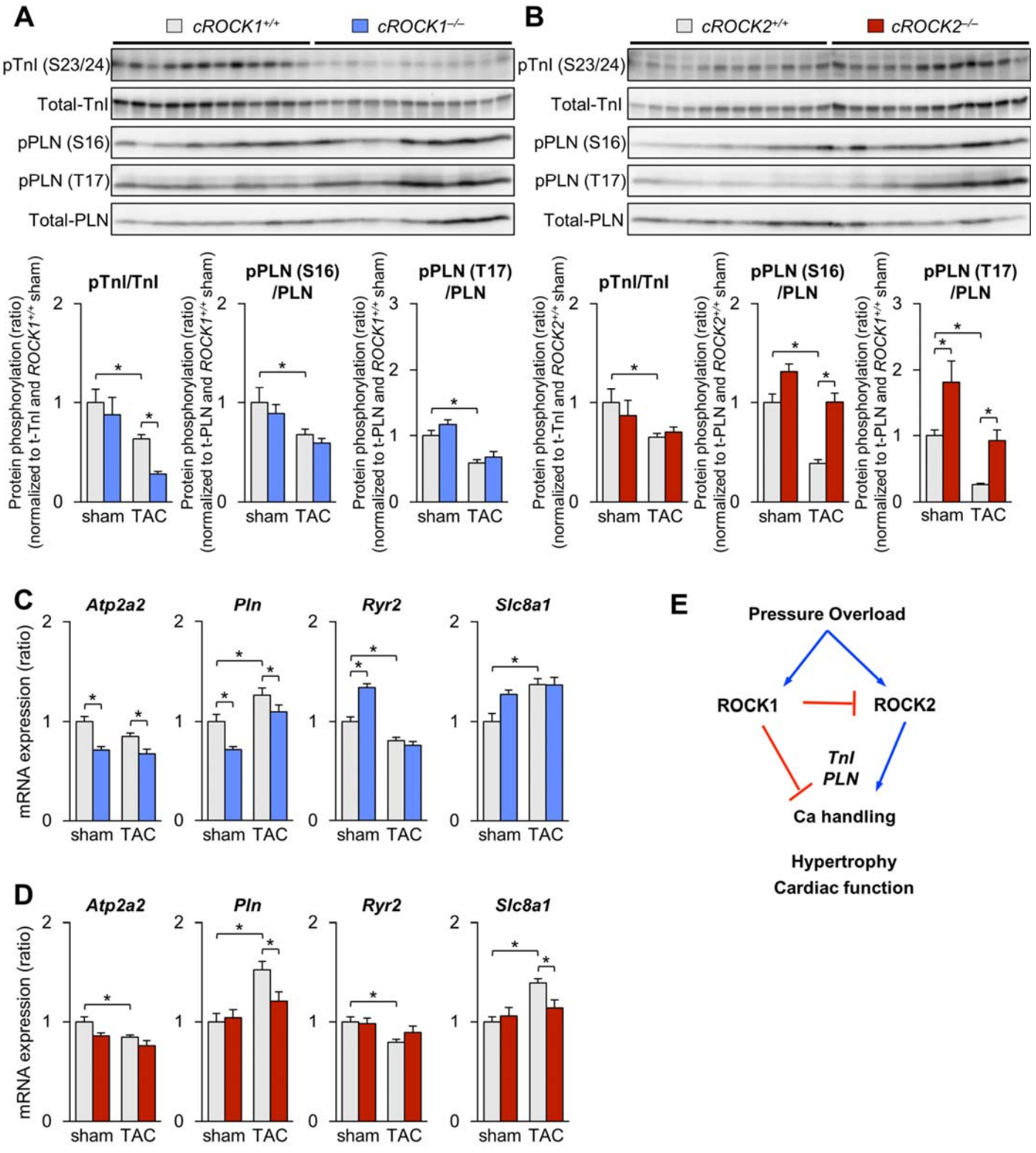
A
cROCK1+/+
cROCK1−/−
pTnI (S23/24)
Total-TnI
pPLN (S16)
pPLN (T17)
Total-PLN
pTnI/TnI
pPLN (S16) /PLN
pPLN (T17) /PLN
Protein phosphorylation (ratio) (normalized to t-TnI and ROCK1+/+ sham)
Protein phosphorylation (ratio) (normalized to t-PLN and ROCK1+/+ sham)
sham TAC
B
cROCK2+/+
cROCK2−/−
Protein phosphorylation (ratio) (normalized to t-TnI and ROCK2+/+ sham)
Protein phosphorylation (ratio) (normalized to t-PLN and ROCK2+/+ sham)
C
Atp2a2
Pln
Ryr2
Slc8a1
mRNA expression (ratio)
D
E
Pressure Overload
ROCK1
ROCK2
TnI
PLN
Ca handling
Hypertrophy
Cardiac function

Figure S8. Different roles of ROCK1 and ROCK2 in Ca^{2+} handling

(**A**) Representative Western blot and quantification of cTnI phosphorylation at Ser23/24, total cTnI, phospholamban phosphorylation (Ser16/Thr17) and total phospholamban in *cROCK1*$^{+/+}$ and *cROCK1*$^{-/-}$ hearts at 4 weeks after transverse aortic constriction (TAC, *n*=12 each) or sham operation (*n*=5 each). (**B**) Representative Western blot and quantification of cTnI phosphorylation at Ser23/24, total cTnI, phospholamban phosphorylation (Ser16/Thr17) and total phospholamban in *cROCK2*$^{+/+}$ and *cROCK2*$^{-/-}$ hearts at 4 weeks after TAC (*n*=12 each) or sham operation (*n*=5 each). (**C**) Relative mRNA expression of SERCA2a (*Atp2a2*), phospholamban (*Pln*), ryanodine receptor 2 (*Ryr2*), and Na^+/Ca^{2+} exchanger 1 (*Slc8a1*), in *cROCK1*$^{+/+}$ and *cROCK1*$^{-/-}$ hearts at 4 weeks after TAC (*n*=12 each) or sham operation (*n*=5 each). (**D**) Relative mRNA expression of *Atp2a2*, *Pln*, *Ryr2*, and *Slc8a1*, in *cROCK2*$^{+/+}$ and *cROCK2*$^{-/-}$ hearts at 4 weeks after TAC (*n*=12 each) or sham operation (*n*=5 each). (**E**) Schematic representation of the different roles of ROCK1 and ROCK2 in cardiomyocytes for Ca^{2+} handling. Data represent the mean ± s.e.m. **P*<0.05. Comparisons of parameters were performed with two-way ANOVA, followed by Tukey's HSD test for multiple comparisons.

Mouse cardiomyocytes (trabeculae)

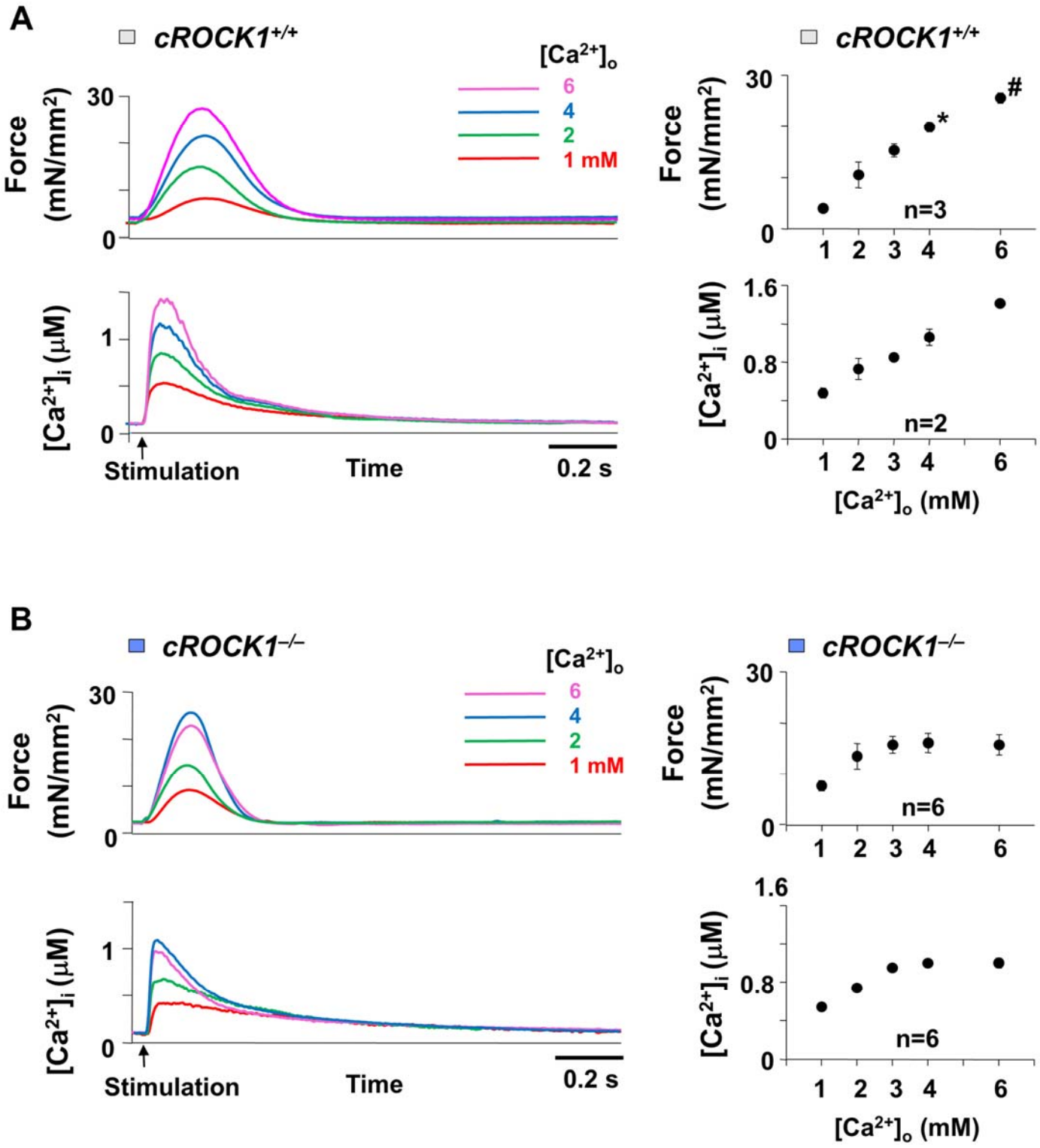

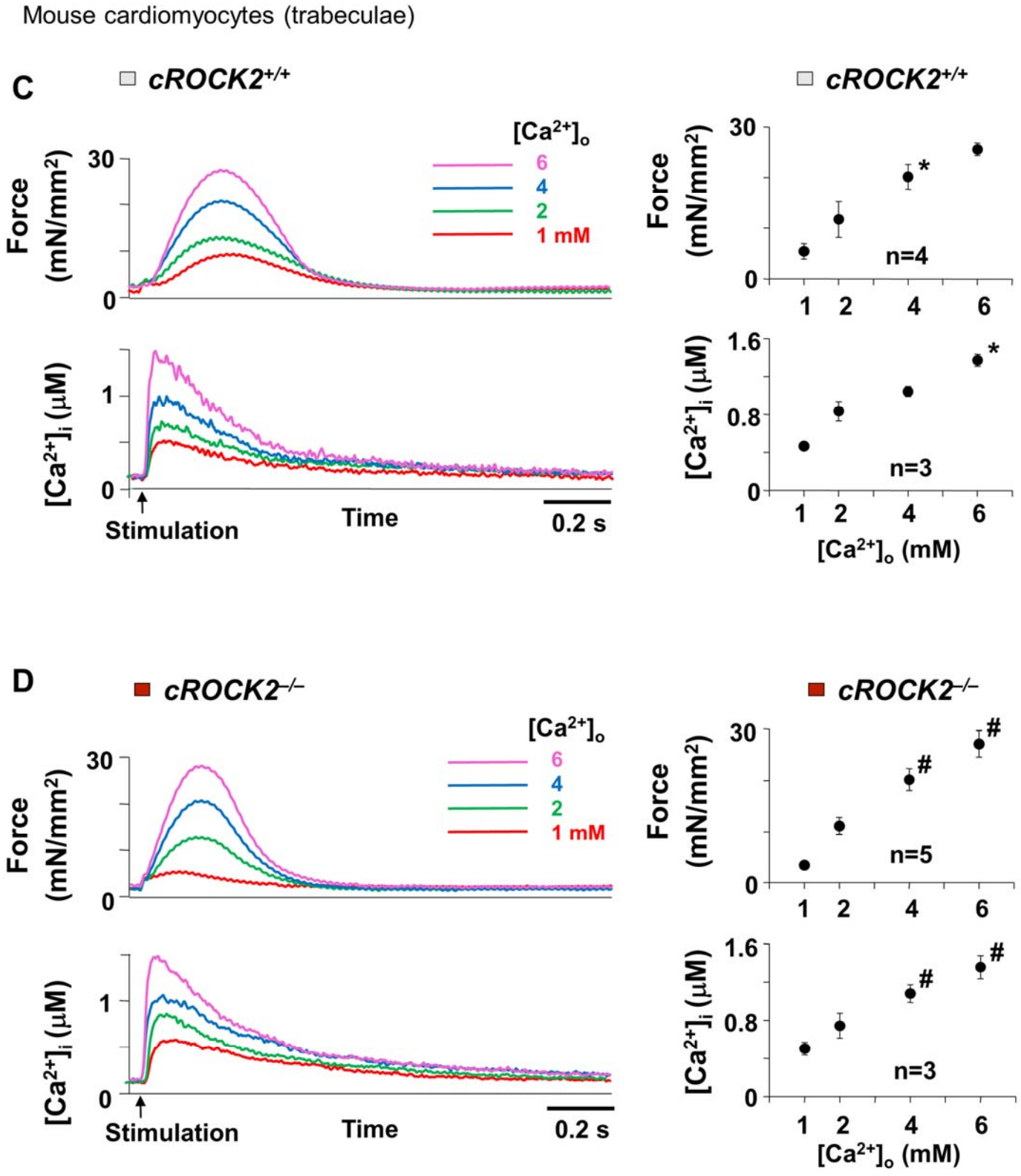
Mouse cardiomyocytes (trabeculae)
C
cROCK2+/+
[Ca2+]o
6
4
2
1 mM
Force (mN/mm2)
30
0
[Ca2+]i (μM)
1
0
Stimulation
Time
0.2 s
cROCK2+/+
Force (mN/mm2)
30
0
n=4
1 2 4 6
[Ca2+]i (μM)
1.6
0.8
0
n=3
1 2 4 6
[Ca2+]o (mM)
D
cROCK2–/–
[Ca2+]o
6
4
2
1 mM
Force (mN/mm2)
30
0
[Ca2+]i (μM)
1
0
Stimulation
Time
0.2 s
cROCK2–/–
Force (mN/mm2)
30
0
n=5
1 2 4 6
[Ca2+]i (μM)
1.6
0.8
0
n=3
1 2 4 6
[Ca2+]o (mM)

Figure S9. Force and intracellular Ca^{2+} concentration in mouse trabeculae

(**A**) Representative tracings of force and $[Ca^{2+}]_i$ by 0.5 Hz electrical stimulation according to different $[Ca^{2+}]_o$ and relations between $[Ca^{2+}]_o$ and force or $[Ca^{2+}]_i$ in the trabeculae from *cROCK1*$^{+/+}$ mice (n=2-3). (**B**) Representative tracings of force and $[Ca^{2+}]_i$ by 0.5 Hz electrical stimulation according to different $[Ca^{2+}]_o$ and relations between $[Ca^{2+}]_o$ and force or $[Ca^{2+}]_i$ in the trabeculae from *cROCK1*$^{-/-}$ mice (n=6). (**C**) Representative tracings of force and $[Ca^{2+}]_i$ by 0.5 Hz electrical stimulation according to different $[Ca^{2+}]_o$ and relations between $[Ca^{2+}]_o$ and force or $[Ca^{2+}]_i$ in the trabeculae from *cROCK2*$^{+/+}$ mice (n=3-4). (**D**) Representative tracings of force and $[Ca^{2+}]_i$ by 0.5 Hz electrical stimulation according to different $[Ca^{2+}]_o$ and relations between $[Ca^{2+}]_o$ and force or $[Ca^{2+}]_i$ in the trabeculae from *cROCK2*$^{-/-}$ mice (n=3-5). Data represent the mean ± s.e.m. *P<0.05 compared with one-step lower $[Ca^{2+}]_o$, $^{\#}P$<0.01 compared with one-step lower $[Ca^{2+}]_o$. Comparisons of parameters were performed with two-way ANOVA, followed by Tukey's HSD test for multiple comparisons.

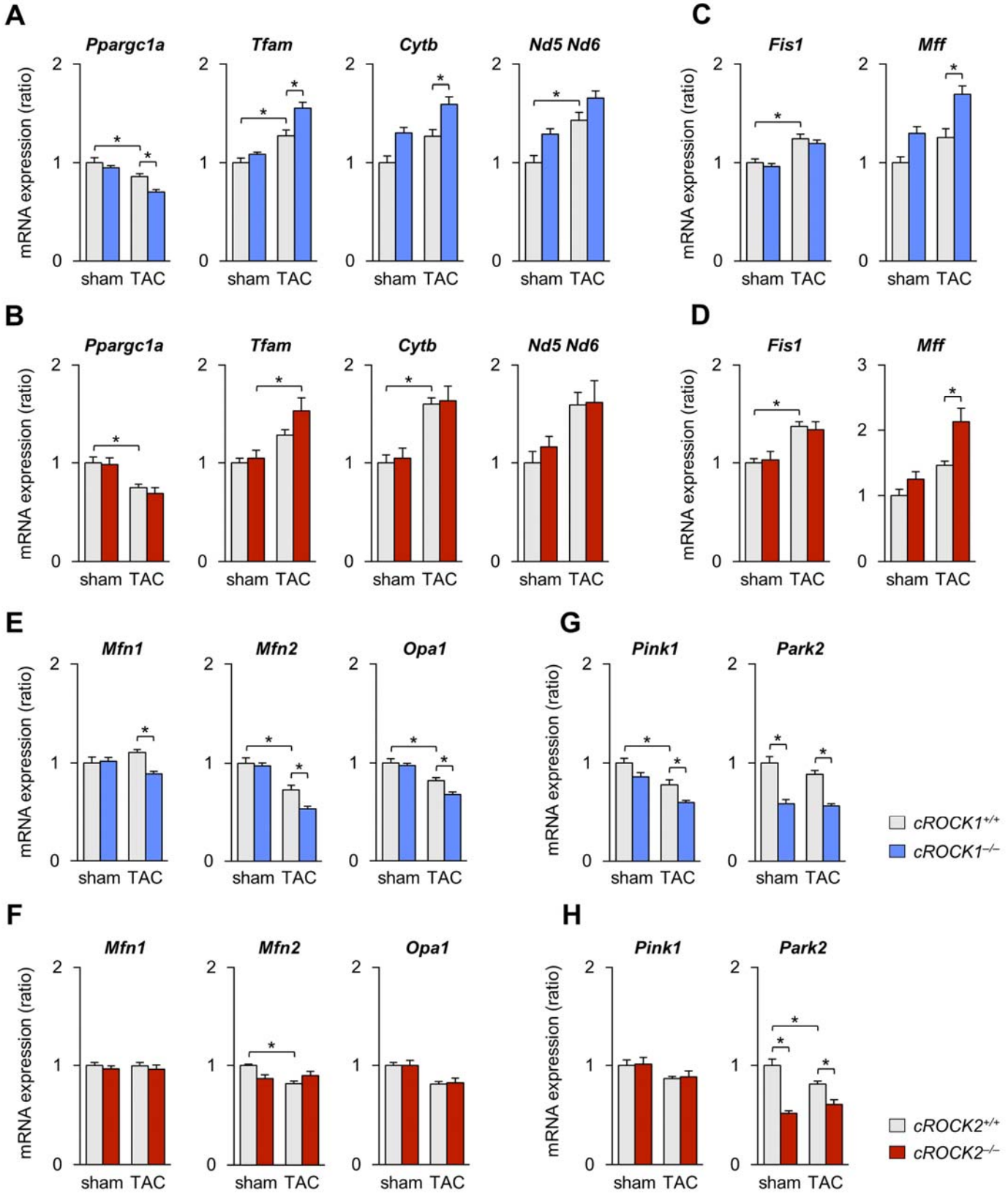
A
Ppargc1a
Tfam
Cytb
Nd5 Nd6
C
Fis1
Mff
B
Ppargc1a
Tfam
Cytb
Nd5 Nd6
D
Fis1
Mff
E
Mfn1
Mfn2
Opa1
G
Pink1
Park2
F
Mfn1
Mfn2
Opa1
H
Pink1
Park2
mRNA expression (ratio)
sham TAC
cROCK1+/+
cROCK1−/−
cROCK2+/+
cROCK2−/−

Figure S10. Expressions of gene related to mitochondrial homeostasis after TAC.
(**A**) Relative mRNA expressions of key molecules concerning mitochondrial biogenesis, such as *Ppargc1a*, *Tfam*, *Cytb* and *Nd5/Nd6* in the hearts of *cROCK1*$^{+/+}$ and *cROCK1*$^{-/-}$ mice at 4 weeks after TAC (*n*=12 each) or sham operation (*n*=5 each). (**B**) Relative mRNA expressions of key molecules concerning mitochondrial biogenesis same as penel (**A**) in the hearts of *cROCK2*$^{+/+}$ and *cROCK2*$^{-/-}$ mice at 4 weeks after transverse aortic constriction (TAC, *n*=12 each) or sham operation (*n*=5 each). (**C**) Relative mRNA expressions of key molecules concerning mitochondrial fission, such as *Fis1* and *Mff* in the hearts of *cROCK1*$^{+/+}$ and *cROCK1*$^{-/-}$ mice at 4 weeks after TAC (*n*=12 each) or sham operation (*n*=5 each). (**D**) Relative mRNA expressions of key molecules concerning mitochondrial fission same as penel (**C**) in the hearts of *cROCK2*$^{+/+}$ and *cROCK2*$^{-/-}$ mice at 4 weeks after TAC (*n*=12 each) or sham operation (*n*=5 each). (**E**) Relative mRNA expressions of key molecules concerning mitochondrial fusion, such as *Mfn1*, *Mfn2* and *Opa1* in the hearts of *cROCK1*$^{+/+}$ and *cROCK1*$^{-/-}$ mice at 4 weeks after TAC (*n*=12 each) or sham operation (*n*=5 each). (**F**) Relative mRNA expressions of key molecules concerning mitochondrial fusion same as penel (**E**) in the hearts of *cROCK2*$^{+/+}$ and *cROCK2*$^{-/-}$ mice at 4 weeks after TAC (*n*=12 each) or sham operation (*n*=5 each). (**G**) Relative mRNA expressions of key molecules concerning mitophagy, such as *Pink1* and *Park2* in the hearts of *cROCK1*$^{+/+}$ and *cROCK1*$^{-/-}$ mice at 4 weeks after TAC (*n*=12 each) or sham operation (*n*=5 each). (**H**) Relative mRNA expressions of key molecules concerning mitophagy same as penel (**G**) in the hearts of *cROCK2*$^{+/+}$ and *cROCK2*$^{-/-}$ mice at 4 weeks after TAC (*n*=12 each) or sham operation (*n*=5 each). Data represent the mean ± s.e.m. **P*<0.05. Comparisons of parameters were performed with two-way ANOVA, followed by Tukey's HSD test for multiple comparisons.

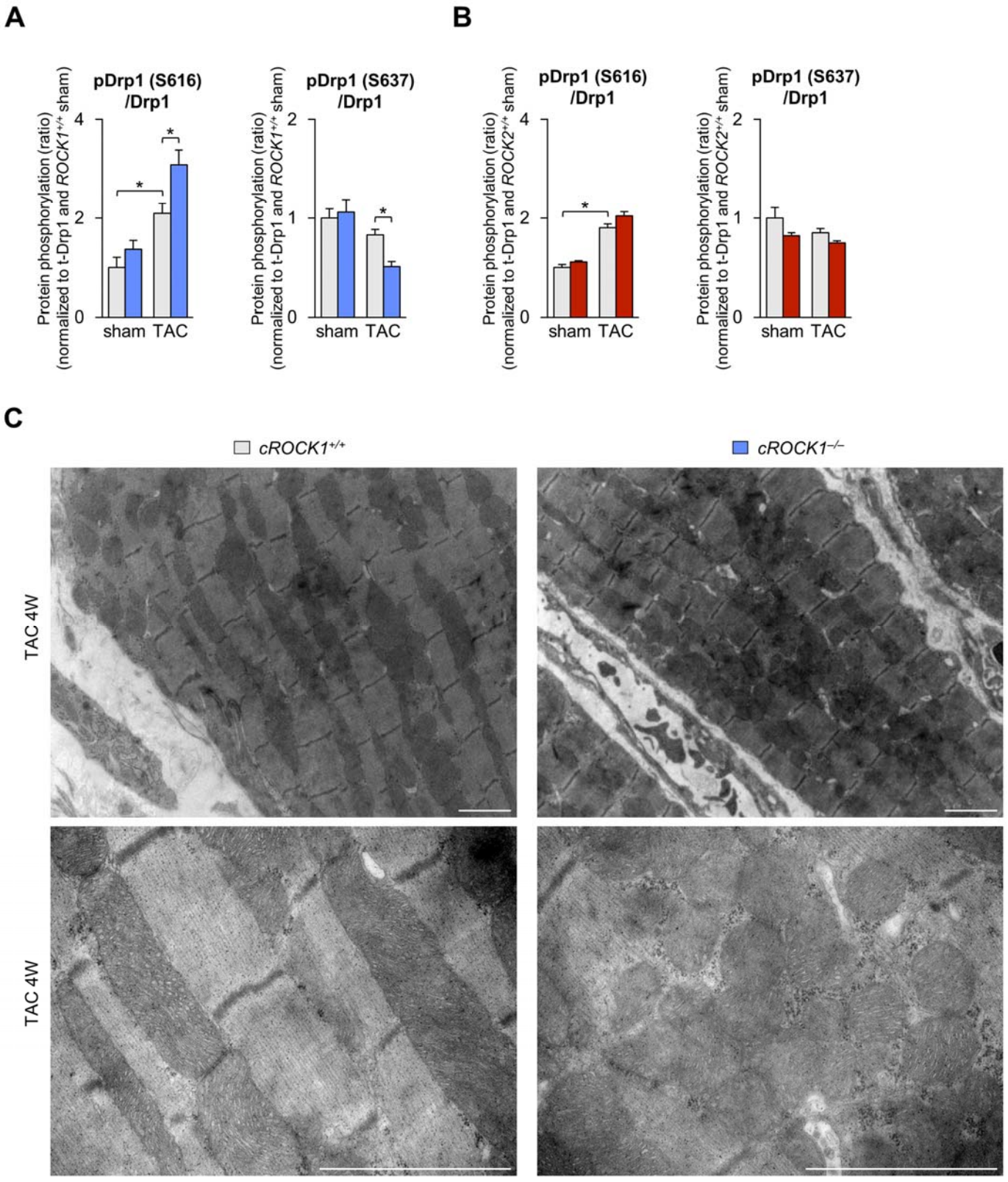
A
pDrp1 (S616) /Drp1
Protein phosphorylation (ratio) (normalized to t-Drp1 and ROCK1+/+ sham)
sham TAC
pDrp1 (S637) /Drp1
B
pDrp1 (S616) /Drp1
Protein phosphorylation (ratio) (normalized to t-Drp1 and ROCK2+/+ sham)
pDrp1 (S637) /Drp1
C
cROCK1+/+
cROCK1−/−
TAC 4W
TAC 4W

Figure S11. Mitochondrial morphology after pressure overload

(**A**) Quantification of Drp1 phosphorylation (Ser616/Ser637) and total Drp1 in *cROCK1*$^{+/+}$ and *cROCK1*$^{-/-}$ hearts at 4 weeks after transverse aortic constriction (TAC, *n*=12 each) or sham operation (*n*=5 each). (**B**) Quantification of Drp1 phosphorylation (Ser616/Ser637) and total Drp1 in *cROCK2*$^{+/+}$ and *cROCK2*$^{-/-}$ hearts at 4 weeks after TAC (*n*=12 each) or sham operation (*n*=5 each). (**C**) Representative transmission electron microscopy images of mitochondria in the left ventricles (LVs) of *cROCK1*$^{+/+}$ and *cROCK1*$^{-/-}$ mice at 4 weeks after TAC. Scale bars, 2 μm. Data represent the mean ± s.e.m. **P*<0.05. Comparisons of parameters were performed with two-way ANOVA, followed by Tukey's HSD test for multiple comparisons.

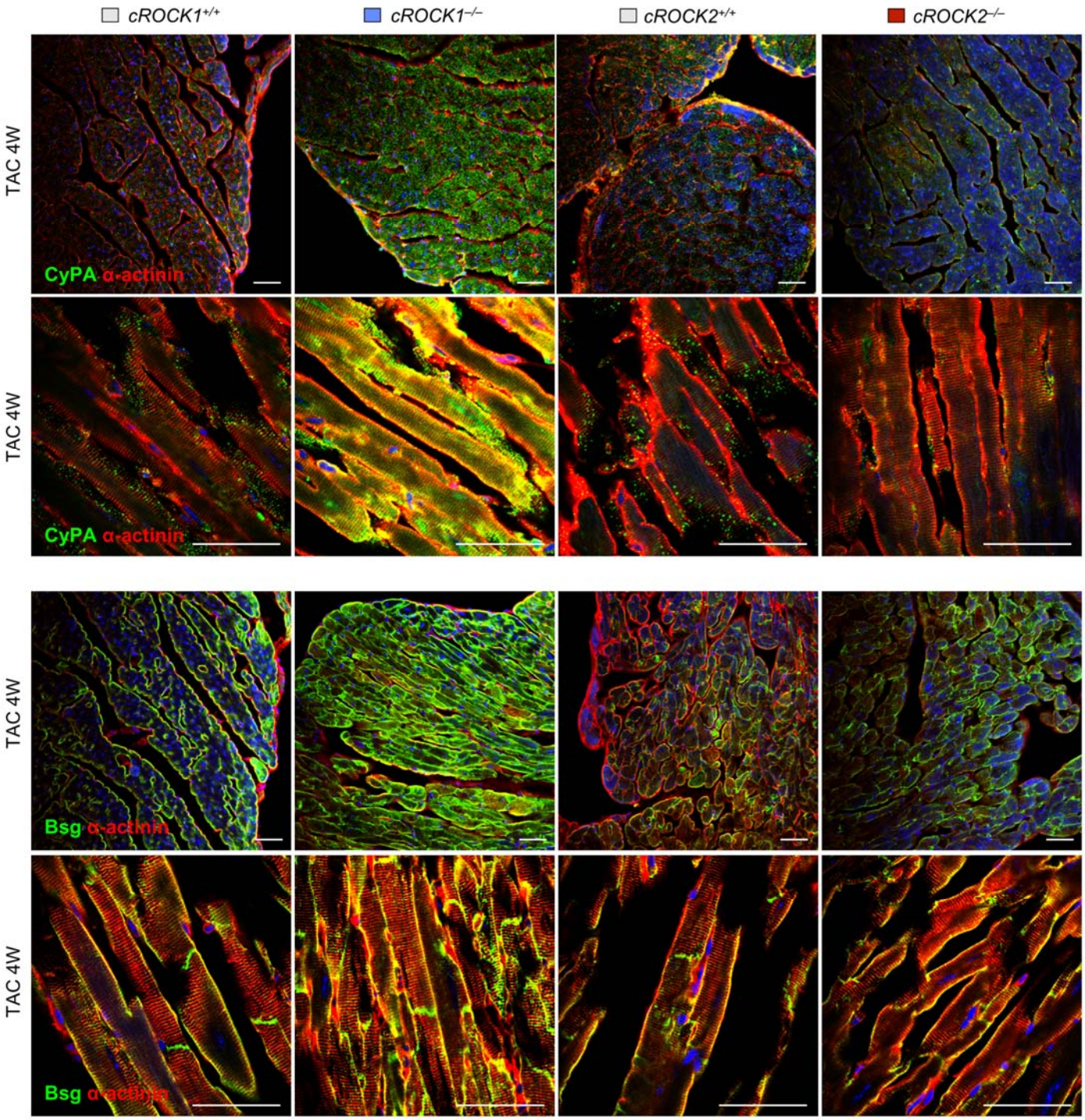

Figure S12. Representative immunostaining showing the localization of cyclophilin A (CyPA, green, Alexa flour 488), basigin (Bsg, green, Alexa flour 488), α-actinin (red, Alexa flour 546) and DAPI in the left ventricles in *cROCK1*$^{+/+}$, *cROCK1*$^{-/-}$, *cROCK2*$^{+/+}$ and *cROCK2*$^{-/-}$ mice at 4 weeks after transverse aortic constriction (TAC). Scale bars, 50μm.

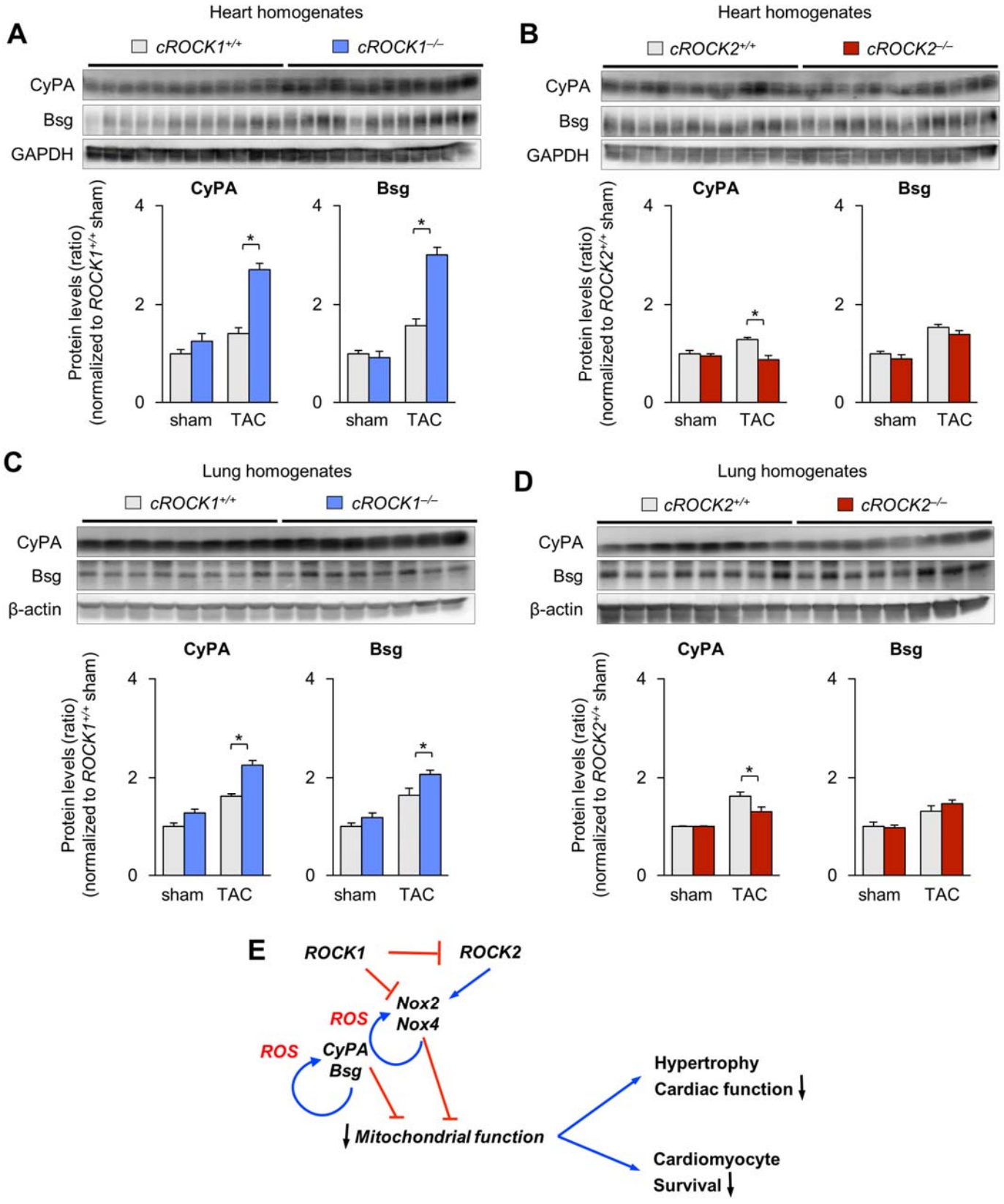
A
Heart homogenates
cROCK1+/+
cROCK1−/−
CyPA
Bsg
GAPDH
CyPA
Bsg
Protein levels (ratio)
(normalized to ROCK1+/+ sham)
sham
TAC
B
Heart homogenates
cROCK2+/+
cROCK2−/−
CyPA
Bsg
GAPDH
Protein levels (ratio)
(normalized to ROCK2+/+ sham)
C
Lung homogenates
cROCK1+/+
cROCK1−/−
CyPA
Bsg
β-actin
D
Lung homogenates
cROCK2+/+
cROCK2−/−
E
ROCK1
ROCK2
Nox2
Nox4
ROS
ROS
CyPA
Bsg
Mitochondrial function
Hypertrophy
Cardiac function
Cardiomyocyte
Survival

Figure S13. Cyclophilin A (CyPA) and basigin (Bsg) in the hearts and lungs after pressure overload

(**A**) Representative Western blot and quantification of CyPA, Bsg and GAPDH in the hearts of *cROCK1*$^{+/+}$ and *cROCK1*$^{-/-}$ mice at 4 weeks after transverse aortic constriction (TAC, *n*=12 each) or sham operation (*n*=5 each). (**B**) Representative Western blot and quantification of CyPA, Bsg and GAPDH in the hearts of *cROCK2*$^{+/+}$ and *cROCK2*$^{-/-}$ mice at 4 weeks after TAC (*n*=12 each) or sham operation (*n*=5 each). (**C**) Representative Western blot and quantification of CyPA, Bsg and β-actin in the lungs of *cROCK1*$^{+/+}$ and *cROCK1*$^{-/-}$ mice at 4 weeks after TAC (*n*=8 each) or sham operation (*n*=4 each). (**D**) Representative Western blot and quantification of CyPA, Bsg and β-actin in the lungs of *cROCK2*$^{+/+}$ and *cROCK2*$^{-/-}$ mice at 4 weeks after TAC (*n*=8 each) or sham operation (*n*=4 each). (**E**) Schematic representation of the augumentation of oxidative stress by CyPA and Bsg as a downstream target of Rho-kinase. Data represent the mean ± s.e.m. **P*<0.05. Comparisons of parameters were performed with two-way ANOVA, followed by Tukey's HSD test for multiple comparisons.

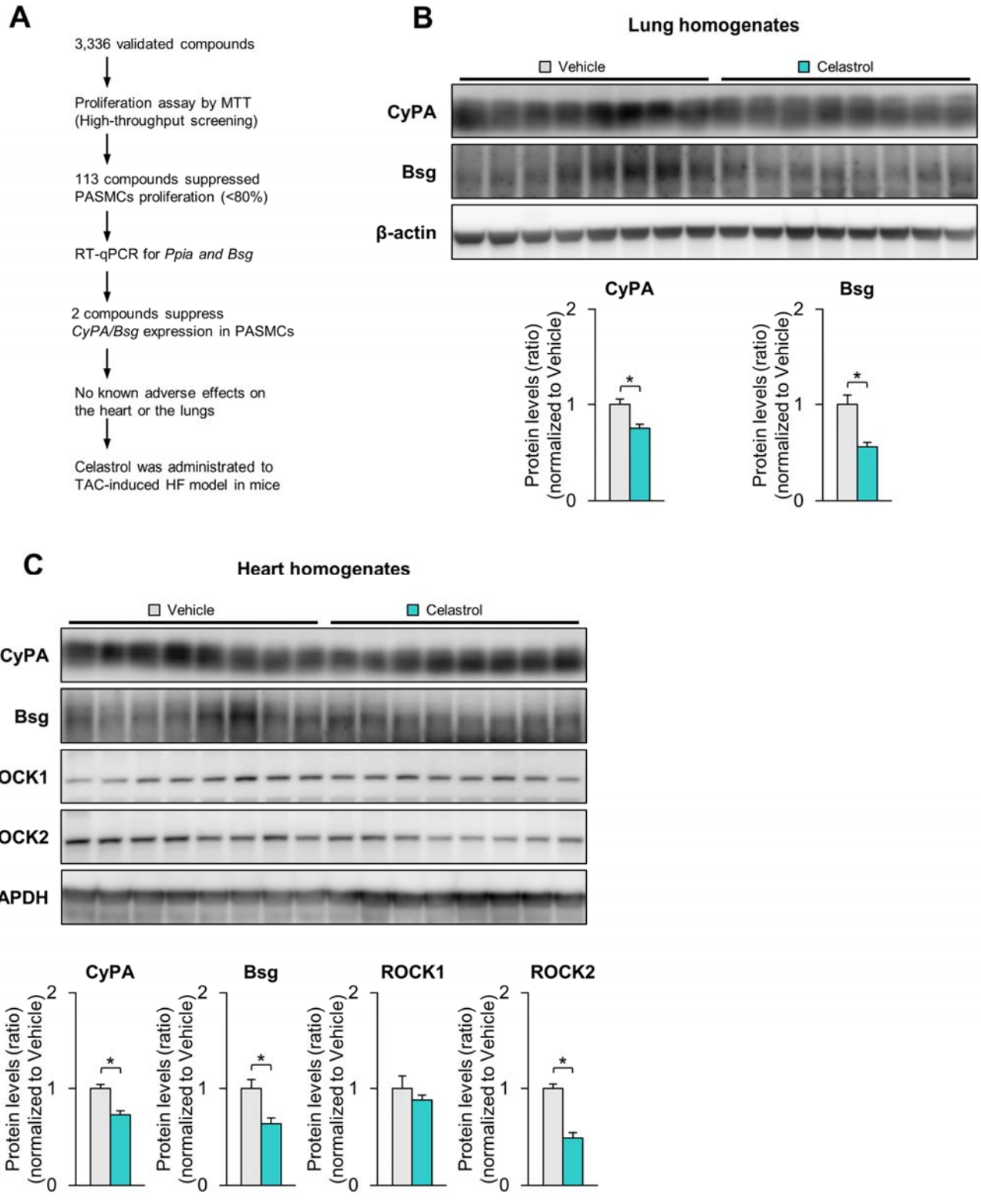
A
3,336 validated compounds
Proliferation assay by MTT
(High-throughput screening)
113 compounds suppressed
PASMCs proliferation (<80%)
RT-qPCR for Ppia and Bsg
2 compounds suppress
CyPA/Bsg expression in PASMCs
No known adverse effects on
the heart or the lungs
Celastrol was administrated to
TAC-induced HF model in mice
B
Lung homogenates
Vehicle
Celastrol
CyPA
Bsg
β-actin
CyPA
Bsg
Protein levels (ratio)
(normalized to Vehicle)
0
1
2
*
C
Heart homogenates
Vehicle
Celastrol
CyPA
Bsg
ROCK1
ROCK2
GAPDH
CyPA
Bsg
ROCK1
ROCK2
Protein levels (ratio)
(normalized to Vehicle)
0
1
2
*

Figure S14. Celastrol ameliorates pressure-overload-induced cardiac dysfunction and post-capillary pulmonary hypertension

(**A**) Schematic outline of high-throughput screening (HTS) to identify compounds that suppress cyclophilin A (CyPA) and basigin (Bsg) expression and proliferation in pulmonary artery smooth muscle cells (PASMCs) from patients with pulmonary arterial hypertension (PAH-PASMCs). First, we treated PAH-PASMCs with 3,336 compounds (5 μM each) for 48 hours and performed a proliferation assay (MTT assay). We identified 113 compounds that suppressed PAH-PASMCs proliferation by more than 20%. We then treated PAH-PASMCs with these 113 compounds (5 μM each) for 4 hours, extracted total RNA to measure the CyPA and Bsg expression by RT-PCR, and found 2 compounds that suppress the expressions of CyPA and Bsg mRNA. MTT, 3-(4,5-di-methylthiazol-2-yl)-2,5-diphenyltetrazolium bromide. (**B**) Representative Western blot and quantification of CyPA, Bsg and β-actin expressions in the lungs after treatment with celastrol or control vehicle for 4 weeks (n=8 each). (**C**) Representative Western blot and quantification of CyPA, Bsg, ROCK1, ROCK2 and GAPDH in the hearts after treatment with celastrol or control vehicle for 4 weeks (n=8 each). Data represent the mean ± s.e.m. *P<0.05. Comparisons of parameters were performed with the unpaired Student's t-test.

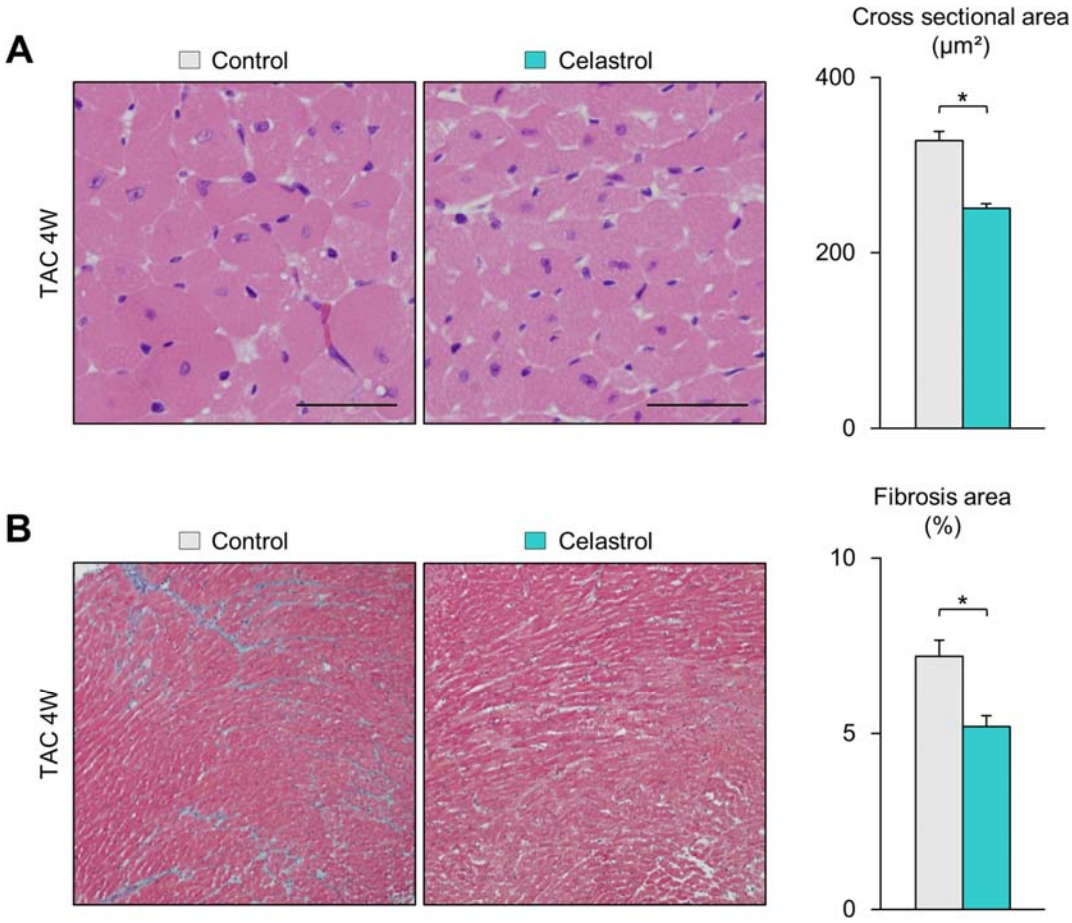

Figure S15. Celastrol attenuates cardiac hypertrophy and fibrosis in mice

(**A**) Left, representative photomicrographs of hematoxylin-eosin (HE) staining of hearts after transverse aortic constriction (TAC). Scale bars, 50 μm. Right, quantitative analysis of cardiomyocyte cross-sectional area (CSA) in mice with or without celastrol treatment after TAC. (**B**) Left, representative photomicrographs of Elastica-Masson (EM) staining of hearts after transverse aortic constriction (TAC). Scale bars, 100 μm. Right, quantitative analysis of interstitial fibrotic area in mice with or without celastrol treatment after TAC. Data represent the mean ± s.e.m. **P*<0.05. Comparisons of parameters were performed with unpaired Student's *t*-test.

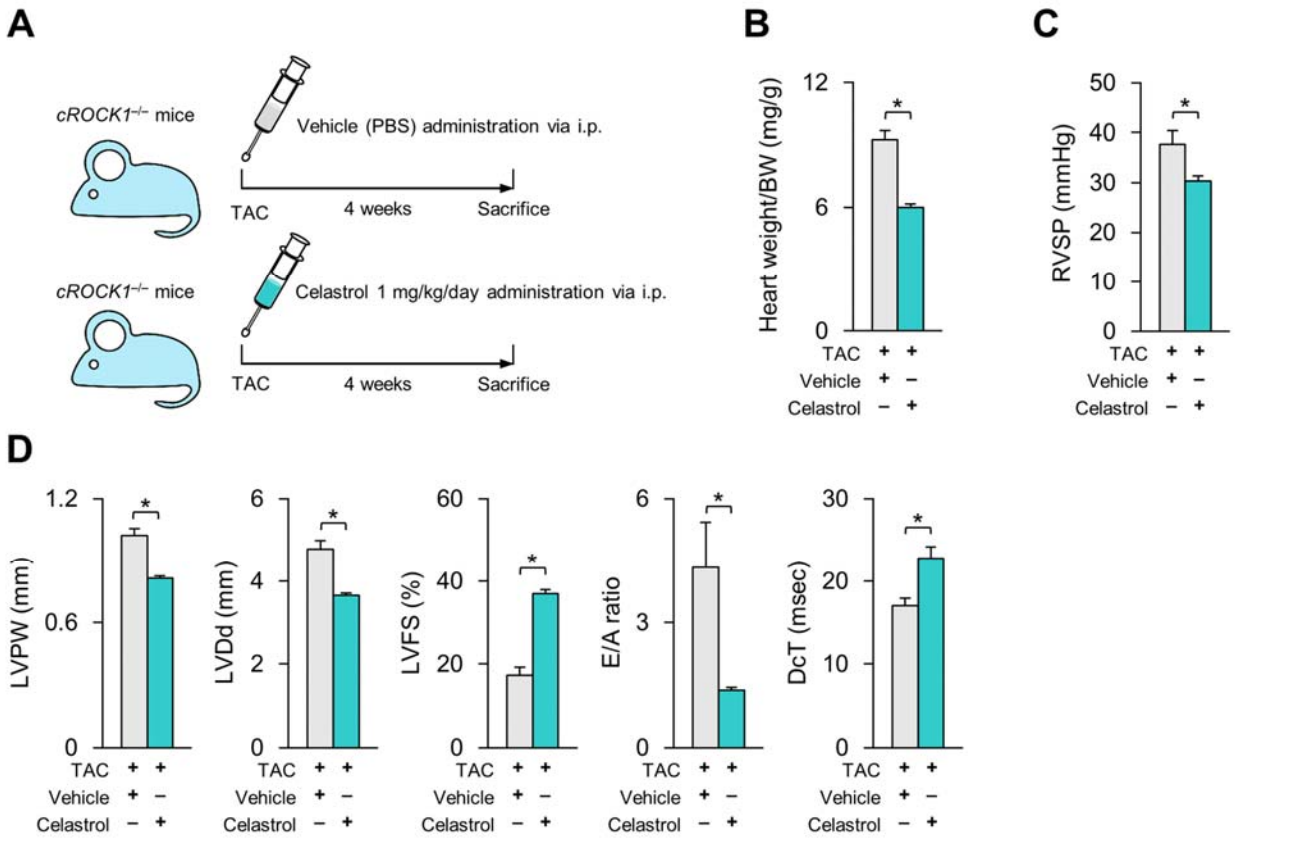

Figure S16. Celastrol ameliorates cardiac dysfunction and post-capillary PH in c*ROCK1*$^{-/-}$ mice

(**A**) Schematic protocols for celastrol administration to *cROCK1*$^{-/-}$ mice subjected to transverse aortic constriction (TAC), in which celastrol (1 mg/kg/day) or control vehicle was administered by intraperitoneal injection. (**B**) The ratio of heart weight/body weight (BW) after treatment with celastrol or control vehicle for 4 weeks (n=9 each). (**C**) Right ventricular systolic pressure (RVSP) after treatment with celastrol or vehicle for 4 weeks (n=9 each). (**D**) Quantitative analysis of the echocardiographic parameters of cardiac function after treatment with celastrol or control vehicle for 4 weeks (n=9 each). Data represent the mean ± s.e.m. *P<0.05. Comparisons of parameters were performed with unpaired Student's t-test.

References

1. Shimizu T, *et al.* (2013) Crucial role of ROCK2 in vascular smooth muscle cells for hypoxia-induced pulmonary hypertension in mice. *Arterioscler Thromb Vasc Biol* 33(12):2780-2791.
2. Asaumi Y, *et al.* (2007) Protective role of endogenous erythropoietin system in nonhematopoietic cells against pressure overload-induced left ventricular dysfunction in mice. *Circulation* 115(15):2022-2032.
3. Ikeda S, *et al.* (2014) Crucial role of Rho-kinase in pressure overload-induced right ventricular hypertrophy and dysfunction in mice. *Arterioscler Thromb Vasc Biol* 34(6):1260-1271.
4. Suzuki K, *et al.* (2016) Basigin promotes cardiac fibrosis and failure in response to chronic pressure overload in mice. *Arterioscler Thromb Vasc Biol* 36(4):636-646.
5. Methawasin M, *et al.* (2016) Experimentally increasing the compliance of titin through RNA binding motif-20 (RBM20) inhibition improves diastolic function in a mouse model of heart failure with preserved ejection fraction. *Circulation* 134(15):1085-1099.
6. Pacher P, Nagayama T, Mukhopadhyay P, Batkai S, Kass DA (2008) Measurement of cardiac function using pressure-volume conductance catheter technique in mice and rats. *Nat Protoc* 3(9):1422-1434.
7. Satoh K, *et al.* (2014) Basigin mediates pulmonary hypertension by promoting inflammation and vascular smooth muscle cell proliferation. *Circ Res* 115(8):738-750.
8. Satoh K, *et al.* (2009) Cyclophilin A enhances vascular oxidative stress and the development of angiotensin II-induced aortic aneurysms. *Nat Med* 15(6):649-656.
9. Funayama A, *et al.* (2013) Cardiac nuclear high mobility group box 1 prevents the development of cardiac hypertrophy and heart failure. *Cardiovasc Res* 99(4):657-664.
10. Takefuji M, *et al.* (2013) RhoGEF12 controls cardiac remodeling by integrating G protein- and integrin-dependent signaling cascades. *J Exp Med* 210(4):665-673.
11. Herum KM, *et al.* (2013) Syndecan-4 signaling via NFAT regulates extracellular matrix production and cardiac myofibroblast differentiation in response to mechanical stress. *J Mol Cell Cardiol* 54:73-81.
12. Kannaiyan R, Shanmugam MK, Sethi G (2011) Molecular targets of celastrol derived from Thunder of God Vine: potential role in the treatment of inflammatory disorders and cancer. *Cancer Lett* 303(1):9-20.
13. Breiman L (1984) *Classification and regression trees* (Wadsworth International Group,

Belmont, Calif.).